CRITICAL SURFACE OF THE 1-2 MODEL

GEOFFREY R. GRIMMETT AND ZHONGYANG LI

ABSTRACT. The 1-2 model on the hexagonal lattice is a model of statistical mechanics in which each vertex is constrained to have degree either 1 or 2. There are three types of edge, and three corresponding parameters a, b, c. It is proved that, when $a \geq b \geq c > 0$, the surface given by $\sqrt{a} = \sqrt{b} + \sqrt{c}$ is critical. The proof hinges upon a representation of the partition function in terms of that of a certain dimer model. This dimer model may be studied via the Pfaffian representation of Fisher, Kasteleyn, and Temperley. It is proved, in addition, that the two-edge correlation function converges exponentially fast with distance when $\sqrt{a} \neq \sqrt{b} + \sqrt{c}$. Many of the results may be extended to periodic models.

1. INTRODUCTION AND BACKGROUND

The 1-2 model on the hexagonal lattice was introduced by Schwartz and Bruck [32] as an intermediary in the calculation of the capacity of a constrained coding system. They expressed the capacity via holographic reductions (see [36]) in terms of the number of perfect matchings (or dimer configurations), and the latter may be studied via the Pfaffian method of Fisher, Kasteleyn, and Temperley [11, 17, 34]. The 1-2 model may be viewed as a model of statistical mechanics of independent interest, and it is related to the Ising model and the dimer model. In the current paper, we study the 1-2 model within this context, and we establish the exact form of the associated critical curve.

A 1-2 configuration on the hexagonal lattice $\mathbb{H} = (\mathbb{V}, \mathbb{E})$ is a subset F of edges such that every vertex is incident with either one or two edges of F. There are three real parameters $a, b, c > 0$, which are associated with the three classes of edges of $\mathbb{H}$. The weight of a configuration on a finite region is the product over vertices v of one of a, b, c chosen according to the edge-configuration at v. (See Figure 2.2.)

Through a sequence of transformations, the 1-2 model turns out to be linked to an enhanced Ising model, a polygon model, and a dimer model. These connections are pursued here, and in the linked paper [15]. The main result (Theorem 3.1) states

Date: 28 June 2015, revised 1 June 2016.

2010 *Mathematics Subject Classification.* 82B20, 60K35, 05C70.

Key words and phrases. 1-2 model, Ising model, dimer model, perfect matching, Kasteleyn matrix.

that, when $a \geq b, c > 0$, the surface given by $\sqrt{a} = \sqrt{b} + \sqrt{c}$ is critical. This is proved by an analysis of the behaviour of the two-edge correlation function $\langle \sigma_e \sigma_f \rangle$ as $|e - f| \to \infty$. The model is called *uniform* if $a = b = c = 1$, and thus the uniform model is not critical in the above sense.

There has been major progress in recent years in the study of two-dimensional Ising models via rhombic tilings and discrete holomorphic observables (see, for example, [4, 6, 7, 20]). There is a rhombic representation of the critical polygon model associated with the 1-2 model, and an associated discrete holomorphic function, but this is not explored here.

Certain properties of the underlying hexagonal lattice are utilized heavily in this work, such as trivalence, planarity, and support of a $\mathbb{Z}^2$ action. It may be possible to extend many of the results of this paper to certain other graphs with such properties, including the Archimedean lattice $(3, 12^2)$ and the square/octagon lattice $(4, 8^2)$. Further extensions are possible to periodic models on hexagonal and other lattices. (See Remarks 3.3, 4.3 and Section 10.2.)

It was shown already in [25] that a (geometric) phase transition exists for the 1-2 model on $\mathbb{H}$. An *a-cluster* is a connected set of vertices each having local weight a (as above). It was shown that there exists, a.s. with respect to any translation-invariant Gibbs measure, no infinite path of present edges. In contrast, for given b, c, there exists no infinite a-cluster for small a, whereas such a cluster exists for large a. The a.s. uniqueness of infinite 'homogeneous' clusters was proved in [27].

This paper is concentrated on the 1-2 model and its dimer representation. A related representation involves the polygon model on $\mathbb{H}$, and the phase transition of the latter model is the subject of the linked paper [15]. The polygon representation is related to the high temperature expansion of the Ising model, and results in an inhomogeneous model that may regarded as an extension of the $O(n)$ model with $n = 1$; see [10] for a recent reference to the $O(n)$ model.

The structure of the current work is as follows. The precise formulation of the 1-2 model appears in Section 2, and the main theorems (Theorems 3.1–3.2) are presented in Section 3.

The 1-2 model is coupled with an Ising model in Section 4, in a manner not dissimilar to the Edwards–Sokal coupling of the random-cluster model (see [14, Sect. 1.4]). It may be transformed into a dimer model (see [25]) as described in Section 5. In Section 6, we gather some conclusions about infinite-volume free energy and infinite-volume measures that are new for the 1-2 model. Theorem 3.1 is proved in Sections 7–8 via an analysis using Pfaffians, and Theorem 3.2 is proved in Sections 4.5 and 9. Section 10 is devoted to extensions of the above results to periodic 1-2 and Ising models to which the Kac–Ward approach of [29] does not appear to apply.

2. The 1-2 model

Let $G = (V, E)$ be a finite graph. A *1-2 configuration* on G is a subset $F \subseteq E$ such that every $v \in V$ is incident to either one or two members of F. The subset F may be expressed as a vector in the space $\Sigma = \{-1, +1\}^E$ where -1 represents an absent edge and $+1$ a present edge. Thus the space of 1-2 configurations may be viewed as the subset of Σ containing all vectors σ such that

$$\sum_{e \ni v} \sigma'_e \in \{1, 2\}, \qquad v \in V,$$

where

$$\sigma'(e) = \tfrac{1}{2}(1 + \sigma(e)). \tag{2.1}$$

(In Section 4.2, we will write Σ^{e} for Σ, in order to distinguish it from a space of vertex-spins to be denoted Σ^{v}.)

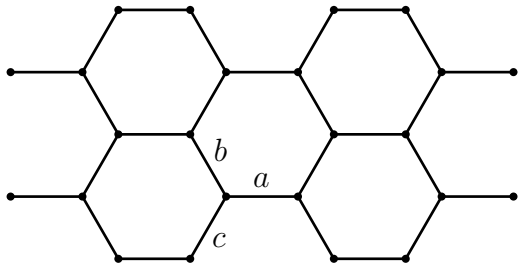

FIGURE 2.1. An embedding of the hexagonal lattice. Horizontal edges are said to be of type a, NW edges of type b, and NE edges of type c.

Suppose now that G is a finite part of the hexagonal lattice $\mathbb{H}$, suitably embedded in $\mathbb{R}^2$, see Figure 2.1. The embedding is such that each edge may be viewed as one of: horizontal, NW, or NE. (Later we shall consider a finite box with toroidal boundary conditions.) Let $a, b, c \geq 0$ be such that $(a, b, c) \neq (0, 0, 0)$, and associate these three parameters with the edges as indicated in the figure. For $\sigma \in \Sigma$ and $v \in V$, let $\sigma|_v$ be the sub-configuration of σ on the three edges incident to v. There are $2^3 = 8$ possible local configurations, which we encode as words of length three in the alphabet with letters $\{0, 1\}$. That is, for $v \in V$, we observe the states $\sigma(e_{v,a}), \sigma(e_{v,b}), \sigma(e_{v,c})$, where $e_{v,a}$, $e_{v,b}$, $e_{v,c}$ are the edges of type a, b, c (respectively) incident to v. The corresponding *signature* s_v is the word $\sigma'(e_{v,c})\sigma'(e_{v,b})\sigma'(e_{v,a})$ of length 3, where σ' is given in (2.1). That is, the signature of v is given as in Figure 2.2, together with the local weight $w(\sigma|_v)$ associated with each of the eight possible signatures.

The hexagonal lattice $\mathbb{H}$ is, of course, bipartite, and we colour the two vertex-classes *black* and *white*. The upper diagrams of Figure 2.2 are for black vertices, and the lower for white vertices.

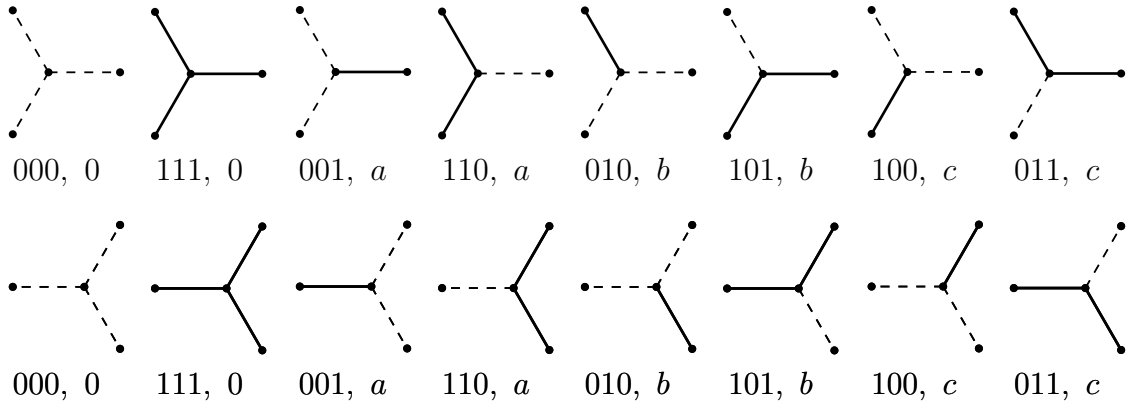

FIGURE 2.2. The eight possible local configurations $\sigma|_v$ at a vertex v in the two cases of *black* and *white* vertices. The signature of each is given, and also the local weight $w(\sigma|_v)$ associated with each instance.

To the vector $\sigma \in \Sigma$, we assign the weight

$$w(\sigma) = \prod_{v \in V} w(\sigma|_v). \tag{2.2}$$

These weights give rise to the partition function

$$Z = \sum_{\sigma \in \Sigma} w(\sigma), \tag{2.3}$$

which leads in turn to the probability measure

$$\mu(\sigma) = \frac{1}{Z} w(\sigma), \qquad \sigma \in \Sigma. \tag{2.4}$$

It is easily seen that the measure μ is invariant under the mapping $(a, b, c) \mapsto (ka, kb, kc)$ with $k > 0$. It is therefore natural to re-parametrize the 1-2 model by

$$(a', b', c') = \frac{(a, b, c)}{\|(a, b, c)\|_2}. \tag{2.5}$$

We will work mostly with a finite subgraph of $\mathbb{H}$ subject to toroidal boundary conditions. Let $n \geq 1$, and let τ_1, τ_2 be the two shifts of $\mathbb{H}$, illustrated in Figure 2.3, that map an elementary hexagon to the next hexagon in the given directions. The pair (τ_1, τ_2) generates a $\mathbb{Z}^2$ action on $\mathbb{H}$, and we write $\mathbb{H}_n$ for the quotient graph of $\mathbb{H}$ under the subgroup of $\mathbb{Z}^2$ generated by τ_1^n and τ_2^n. The resulting $\mathbb{H}_n$ is illustrated in Figure 2.3, and may be viewed as a finite subgraph of $\mathbb{H}$ subject to toroidal boundary conditions.

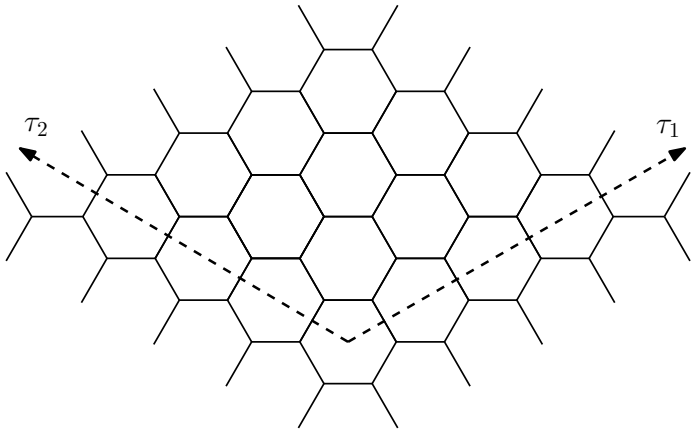

FIGURE 2.3. The graph $\mathbb{H}_n$ is an $n \times n$ 'diamond' wrapped onto a torus, as illustrated here with $n = 4$.

Our purpose in this paper is to study the 1-2 measure (2.4) on $\mathbb{H}_n$ in the infinite-volume limit as $n \to \infty$, and to identify its critical surface. As an indicator of phase transition, we shall use the two-point function $\langle \sigma_e \sigma_f \rangle_n$, where e, f are two edges and $\langle \cdot \rangle_n$ denotes expectation.

We do not explore in detail the nature and multiplicity of infinite-volume measures in this paper. There are certain complexities in such issues arising from the absence of a correlation inequality, and some partial results along these lines may be found in [25, Thm 0.1]. These results are developed in Section 6, where the main result of current value is the existence of the infinite-volume limit of the toroidal 1-2 measure, see Theorem 6.2.

3. MAIN RESULTS

Consider the 1-2 model on $\mathbb{H}_n$ with parameters $a, b, c > 0$. We write $e = \langle x, y \rangle$ for the edge e with endpoints x, y, and we use $\langle X \rangle_n$ to denote expectation of the random variable X with respect to the probability measure of (2.4) on $\mathbb{H}_n$. We shall make use of a measure of distance $|e - f|$ between e and f, and it is largely immaterial which measure we take. For definiteness, consider $\mathbb{H}$ embedded in $\mathbb{R}^2$ in the manner of Figure 2.3, with unit edge-lengths, and let $|e - f|$ be the Euclidean distance between their midpoints.

Theorem 3.1. *Let $a, b, c > 0$, and $e, f \in \mathbb{E}$.*

(a) *The limit $\langle \sigma_e \sigma_f \rangle = \lim_{n \to \infty} \langle \sigma_e \sigma_f \rangle_n$ exists.*

Let $e, f \in \mathbb{E}$ be NW edges such that:

$$\text{there exists a path } \pi = \pi(e,f) \text{ of } \mathbb{H}_n \text{ from } e \text{ to } f \text{ using only horizontal and NW half-edges.} \tag{3.1}$$

(b) *Let $a \geq b > 0$. For almost every $c > 0$ satisfying either $\sqrt{a} > \sqrt{b} + \sqrt{c}$ or $\sqrt{c} > \sqrt{a} + \sqrt{b}$, we have that $\lim_{|e-f|\to\infty} \langle \sigma_e \sigma_f \rangle^2$ exists and is non-zero.*
(c) *If $a \geq b > 0$ and $\sqrt{a} - \sqrt{b} < \sqrt{c} < \sqrt{a} + \sqrt{b}$, then $\langle \sigma_e \sigma_f \rangle \to 0$ as $|e-f| \to \infty$.*
(d) *The convergence in parts* (b) *and* (c) *is exponentially fast in the distance $|e-f|$.*

The two-edge function $\langle \sigma_e \sigma_f \rangle$ behaves in a qualitatively different manner depending on whether or not $\sqrt{a} - \sqrt{b} < \sqrt{c} < \sqrt{a} + \sqrt{b}$. Here is a motivation for condition (3.1). Consider the 'ground states' when either $c = 0$ or $a = b = 0$. By examination of the different cases in Figure 2.2, we may see, subject to (3.1), that

$$\langle \sigma_e \sigma_f \rangle = 1 \qquad \text{if either} \quad a, b > 0,\ c = 0, \quad \text{or} \quad a = b = 0,\ c > 0. \tag{3.2}$$

The result of part (b) will follow from this by an argument using analyticity (and, moreover, the set of c at which the conclusion of (b) fails is a union of isolated points). The theorem remains true with e, f assumed to be horizontal rather than NW.

Theorem 3.1 is not of itself a complete picture of the location of critical phenomena of the 1-2 model, since the conditions on the parameters are allied to the direction of the vector from e to f. (The direction NW is privileged in the above theorem. Similar results hold for the other two lattice directions with suitable permutations of the parameters.) We have not ruled out the theoretical possibility of further critical surfaces in the parameter-space $[0, \infty)^3$, although we have a stronger result for the subcritical phase of Theorem 3.1(c) that does not hinge on condition (3.1).

Theorem 3.2. *Let $a \geq b > 0$ and $\sqrt{a} - \sqrt{b} < \sqrt{c} > \sqrt{a} + \sqrt{b}$. There exists $\alpha(a, b, c) > 0$ such that*

$$\langle \sigma_e \sigma_f \rangle \leq e^{-\alpha |e-f|}, \qquad e, f \in \mathbb{E}. \tag{3.3}$$

Remark 3.3. *The last theorem is a strengthening of Theorem 3.1(c, d) to all directions. Its quickest proof (given in Section 4.5) is based on a result of* [29] *that imposes a condition on the parameters of edges incident to a vertex v, uniformly in v. This condition is satisfied in the current setting (see Section 4.5). In the more general setting of certain periodic but non-constant families of parameters, or possibly of the 1-2 model on other graphs such as the square/octagon lattice, much of Theorem 3.1 remains true, but the condition of* [29] *does not generally hold. In order to overcome this lacuna for more general systems, we present a further proof of Theorem 3.2 in Section 9 (in the slightly more general form of Theorem 9.1) using the dimer-related*

techniques of the proof of Theorem 3.1. Such results may be extended in part to more general periodic settings, see Section 10.2.

The proof of the Theorem 3.1 utilizes a sequence of transformations between the 1-2 model and the Ising and dimer models, as described in the forthcoming sections. Theorem 3.1(a, b, c) is proved in Section 7, with part (d) proved in Section 8. The proof of Theorem 3.2 is presented in Section 4.5.

4. Spin representations of the 1-2 model

Two spin representations of the 1-2 model are presented here. In the first, the 1-2 partition function is rewritten in terms of edge-spins. The second is reminiscent of the random-cluster representation of the Potts model. A further set of spin-variables are introduced at the vertices of the graph, together with an Ising-type partition function.

4.1. **The 1-2 model as a spin system.** Let $\mathbb{H}_n = (V_n, E_n)$ be the quotient hexagonal lattice embedded in the torus in the manner of Figure 2.3. Let $\Sigma = \{-1, +1\}^{E_n}$, where -1 (respectively, $+1$) represents an absent edge (respectively, present edge).

For $\sigma \in \Sigma$ and $v \in V_n$, let $\sigma_{v,a}$, $\sigma_{v,b}$, $\sigma_{v,c}$ denote the spins on the incident a-edge, b-edge, c-edge of v. Two partition functions Z, Z' generate the same measure whenever they differ only in a multiplicative factor (that is, their weight functions satisfy $w(\sigma) = cw'(\sigma)$ for some $c \neq 0$ and all $\sigma \in \Sigma$), in which case we write $Z \doteq Z'$. We represent the 1-2 model as a spin system as follows.

Proposition 4.1. *Let $a, b, c \geq 0$ such that $(a, b, c) \neq (0, 0, 0)$. The 1-2 model with parameters a, b, c on $\mathbb{H}_n$ has partition function Z_n satisfying $Z_n \doteq Z_n'$ where*

$$Z_n' := \sum_{\sigma \in \Sigma} \prod_{v \in V_n} \left(1 + A\sigma_{v,b}\sigma_{v,c} + B\sigma_{v,a}\sigma_{v,c} + C\sigma_{v,a}\sigma_{v,b}\right), \tag{4.1}$$

and

$$A = \frac{a-b-c}{a+b+c}, \quad B = \frac{b-a-c}{a+b+c}, \quad C = \frac{c-a-b}{a+b+c}. \tag{4.2}$$

Proof. By examination of (4.1), we see that a vertex with local configuration labelled a in Figure 2.2 has weight

$$1 + A - B - C = \frac{4a}{a+b+c},$$

with similar expressions for vertices with the other possible signatures. This is in agreement with (2.2)–(2.3), and the claim follows. □

4.2. **Coupled Ising representation.** Let $A\mathbb{H}_n = (AV_n, AE_n)$ be the graph derived from $\mathbb{H}_n = (V_n, E_n)$ by adding a vertex at the midpoint of each edge in E_n. Let $ME_n = \{Me : e \in E_n\}$ be the set of such midpoints, and $AV_n = V_n \cup ME_n$. The edges AE_n are precisely the half-edges of E_n, each being of the form $\langle v, Me\rangle$ for some $v \in V_n$ and incident edge $e \in E_n$.

We introduce an Ising-type model on the graph $A\mathbb{H}_n$. The marginal of the model on midpoints ME_n is a 1-2 model, and the marginal on V_n is an Ising model. This enhanced Ising model is reminiscent of the coupling of the Potts and random-cluster measures, see [14, Sect. 1.4]. It is constructed initially via a weight function on configuration space, and via the associated partition function. The weights may be complex-valued, and thus there does not always exist an associated probability measure.

The better to distinguish between V_n and ME_n, we set $\Sigma^{\mathrm{e}} = \{-1, +1\}^{ME_n}$ as before, and $\Sigma^{\mathrm{v}} = \{-1, +1\}^{V_n}$. An edge $e \in E_n$ is identified with the element of ME_n at its centre. A spin-vector is a pair $(\sigma^{\mathrm{e}}, \sigma^{\mathrm{v}}) \in \Sigma^{\mathrm{e}} \times \Sigma^{\mathrm{v}}$ with $\sigma^{\mathrm{e}} = (\sigma_{v,s} : v \in V_n,\ s = a, b, c)$ and $\sigma^{\mathrm{v}} = (\sigma_v : v \in V_n)$, to which we allocate the (possibly negative, or even complex) weight

$$\prod_{v \in V_n} (1 + \epsilon_a \sigma_v \sigma_{v,a})(1 + \epsilon_b \sigma_v \sigma_{v,b})(1 + \epsilon_c \sigma_v \sigma_{v,c}), \tag{4.3}$$

where $\epsilon_a, \epsilon_b, \epsilon_c \in \mathbb{C}$ are constants associated with horizontal, NW, and NE edges, respectively, and $\sigma_{v,a}, \sigma_{v,b}, \sigma_{v,c}$ denote the spins on midpoints of the corresponding edges incident to $v \in V_n$. If u and v are endpoints of the same edge $\langle u, v\rangle$ of $\mathbb{H}_n$, then $\sigma_{u,a} = \sigma_{v,a}$. In (4.3), each factor $1 + \epsilon_s \sigma_v \sigma_{v,s}$ $(s = a, b, c)$ corresponds to a half-edge of $\mathbb{H}_n$. Recalling that

$$e^{x\sigma_1\sigma_2} = (1 + \sigma_1\sigma_2 \tanh x) \cosh x, \qquad x \in \mathbb{R},\ \sigma_1\sigma_2 = \pm 1, \tag{4.4}$$

the above spin system is a ferromagnetic Ising model on $A\mathbb{H}_n$ when $\epsilon_a, \epsilon_b, \epsilon_c \in (0, 1)$.

4.3. **Marginal on the midpoints ME_n.** The partition function of (4.3) is

$$Z_n(I) := \sum_{\sigma^{\mathrm{e}} \in \Sigma^{\mathrm{e}}} \sum_{\sigma^{\mathrm{v}} \in \Sigma^{\mathrm{v}}} \prod_{v \in V_n} (1 + \epsilon_a \sigma_v \sigma_{v,a})(1 + \epsilon_b \sigma_v \sigma_{v,b})(1 + \epsilon_c \sigma_v \sigma_{v,c}). \tag{4.5}$$

The product, when expanded, is a sum of monomials in which each σ_v has a power between 0 and 3. On summing over σ^{v}, only terms with even powers of the site-spins σ_v survive, and furthermore $\sigma_v^2 = 1$, so that

$$Z_n(I) = \sum_{\sigma^{\mathrm{e}} \in \Sigma^{\mathrm{e}}} \prod_{v \in V_n} \big(1 + \epsilon_b \epsilon_c \sigma_{v,b} \sigma_{v,c} + \epsilon_a \epsilon_c \sigma_{v,a} \sigma_{v,c} + \epsilon_a \epsilon_b \sigma_{v,a} \sigma_{v,b}\big).$$

Let $a, b, c > 0$ be such that $ABC \neq 0$ where A, B, C are given by (4.2), and let

$$\epsilon_a = \sqrt{\frac{BC}{A}}, \quad \epsilon_b = \sqrt{\frac{AC}{B}}, \quad \epsilon_c = \sqrt{\frac{AB}{C}}. \tag{4.6}$$

By (4.1),

$$Z_n(I) = Z'_n, \tag{4.7}$$

whence the marginal model of (4.3) on the midpoints of edges of $\mathbb{H}_n$, subject to (4.6), is simply the 1-2 model with parameters a, b, c.

4.4. **Marginal on the vertices V_n.** This time we perform the sum over σ^{e} in (4.5). Let $g = \langle u, v\rangle \in E_n$ be an edge with weight ϵ_g. We have

$$\sum_{\sigma_g = \pm 1} (1 + \epsilon_g \sigma_u \sigma_g)(1 + \epsilon_g \sigma_v \sigma_g) = 2\left(1 + \epsilon_g^2 \sigma_u \sigma_v\right), \tag{4.8}$$

$$\sum_{\sigma_g = \pm 1} \sigma_g (1 + \epsilon_g \sigma_u \sigma_g)(1 + \epsilon_g \sigma_v \sigma_g) = 2\epsilon_g(\sigma_u + \sigma_v). \tag{4.9}$$

By (4.5) and (4.8),

$$Z_n(I) = 2^{|E_n|} \sum_{\sigma^{\mathrm{v}} \in \Sigma^{\mathrm{v}}} \prod_{g = \langle u,v\rangle \in E_n} \left(1 + \epsilon_g^2 \sigma_u \sigma_v\right). \tag{4.10}$$

By (4.4), this is the partition function of an Ising model on $\mathbb{H}_n$ with (possibly complex) weights.

Let $e = \langle u, v\rangle$, $f = \langle x, y\rangle$ be distinct edges in E_n. Motivated by Section 4.3 and the discussion of the two-edge correlation $\langle \sigma_e \sigma_f \rangle_n$ of the 1-2 model, we define

$$\sigma(e, f) = \frac{1}{Z_n(I)} \sum_{\sigma^{\mathrm{e}} \in \Sigma^{\mathrm{e}}} \sum_{\sigma^{\mathrm{v}} \in \Sigma^{\mathrm{v}}} \sigma_e \sigma_f \prod_{v \in V_n} (1 + \epsilon_a \sigma_v \sigma_{v,a})(1 + \epsilon_b \sigma_v \sigma_{v,b})(1 + \epsilon_c \sigma_v \sigma_{v,c}). \tag{4.11}$$

By (4.9)–(4.10), this equals

$$\begin{aligned} &\frac{1}{Z_n(I)} 2^{|E_n|} \sum_{\sigma^{\mathrm{v}} \in \Sigma^{\mathrm{v}}} \frac{\epsilon_e(\sigma_u + \sigma_v)\epsilon_f(\sigma_x + \sigma_y)}{\left(1 + \epsilon_e^2 \sigma_u \sigma_v\right)\left(1 + \epsilon_f^2 \sigma_x \sigma_y\right)} \prod_{g = \langle u,v\rangle \in E_n} \left(1 + \epsilon_g^2 \sigma_u \sigma_v\right) \\ &\qquad = \sum_{\sigma^{\mathrm{v}} \in \Sigma^{\mathrm{v}}} D_{e,f}(\sigma^{\mathrm{v}}) w(\sigma^v) \Big/ \sum_{\sigma^{\mathrm{v}} \in \Sigma^{\mathrm{v}}} w(\sigma^{\mathrm{v}}), \end{aligned} \tag{4.12}$$

where

$$w(\sigma^{\mathrm{v}}) = \prod_{g=\langle u,v\rangle\in E_n} \left(1+\epsilon_g^2\sigma_u\sigma_v\right),$$

$$D_{e,f}(\sigma^{\mathrm{v}}) = \frac{\epsilon_e(\sigma_u+\sigma_v)\epsilon_f(\sigma_x+\sigma_y)}{\left(1+\epsilon_e^2\sigma_u\sigma_v\right)\left(1+\epsilon_f^2\sigma_x\sigma_y\right)}, \qquad e=\langle u,v\rangle,\ f=\langle x,y\rangle.$$

We interpret $D_{e,f}(\sigma^{\mathrm{v}})$ as 0 when its denominator is 0. Since $\sigma_1+\sigma_2=0$ when $\sigma_1\sigma_2=-1$, we may write

$$D_{e,f}(\sigma^{\mathrm{v}}) = \frac{\epsilon_e(\sigma_u+\sigma_v)\epsilon_f(\sigma_x+\sigma_y)}{(1+\epsilon_e^2)(1+\epsilon_f^2)}. \tag{4.13}$$

If the weights $w(\sigma^{\mathrm{v}})$ are positive (which they are not in general), the ratio on the right side of (4.12) may be interpeted as an expectation. This observation will be used in Section 4.5.

By inspection of (4.10), if $\epsilon_g^2=\pm1$ for some $g\in\{a,b,c\}$, then zero mass is placed on configurations σ for which there exists an edge $\langle u,v\rangle$ of type g with $\sigma_u\sigma_v=\mp1$. We turn to the special case of (4.6) and (4.2) with $ABC\neq0$. Then

$$\epsilon_a^2 = \begin{cases} -1 & \text{if and only if } a^2=b^2+c^2,\\ 1 & \text{if and only if } bc=0,\end{cases} \tag{4.14}$$

and similarly for ϵ_b, ϵ_c. Note in this case that $\sigma(e,f)=\langle\sigma_e\sigma_f\rangle_n$, the two-edge function for the associated 1-2 model.

4.5. **Proof of Theorem 3.2.** Let $e=\langle u,v\rangle$, $f=\langle x,y\rangle$ be distinct edges in E_n such that u, x are white and v, y are black. By (4.11)–(4.13),

$$\langle\sigma_e\sigma_f\rangle_n = \left\langle D_{e,f}(\sigma^{\mathrm{v}})\right\rangle_n^{\mathrm{I}}. \tag{4.15}$$

Recall that the Ising model of (4.10) may have complex weights.

By [29, Cor. 2.5] and known results for the Kac–Ward operator (see [5, 16, 28]), we have that $\langle\sigma_e\sigma_f\rangle := \lim_{n\to\infty}\langle\sigma_e\sigma_f\rangle_n \to 0$ exponentially fast as $|e-f|\to\infty$, so long as the three acute angles with tangents $|\epsilon_g^2|$, $g=a,b,c$, have sum θ satisfying $\theta<\frac{1}{2}\pi$.

Let $a\geq b,c>0$ satisfy $\sqrt{a}<\sqrt{b}+\sqrt{c}$. Suppose first that

$$a\neq b+c. \tag{4.16}$$

Let A, B, C be given by (4.2) and (4.6), so that $A\in(-1,1)\setminus\{0\}$ and $B,C<0$. Note that the ϵ_g of (4.6) are purely imaginary if $A<0$, and real otherwise. Now,

$$\tan\theta = |ABC|\frac{A^{-2}+B^{-2}+C^{-2}}{1-A^2-B^2-C^2}, \tag{4.17}$$

which is strictly positive if

$$A^2 + B^2 + C^2 < 1. \tag{4.18}$$

Using (4.2), it is a short calculation to see that (4.18) holds if (4.16) holds and in addition $a^2 + b^2 + c^2 - 2ab - 2bc - 2ca < 1$, which is to say that $\sqrt{a} < \sqrt{b} + \sqrt{c}$. (See also the proof of Proposition 5.1.) This establishes (3.3) subject to (4.16).

Suppose finally that $a = b + c$, so that $A = 0$ and $B, C < 0$, $B + C = -1$. It is useful to represent the 1-2 model as a polygon model, via its high-temperature expansion. As explained in [15], the two-edge function satisfies

$$\langle \sigma_e \sigma_f \rangle_n = \frac{Z_{n,e\leftrightarrow f}}{Z_n(P)},$$

where $Z_{n,e\leftrightarrow f}$ and $Z_n(P)$ are given at [15, eqns (2.3), (2.7)] with

$$\epsilon_b \epsilon_c = A, \quad \epsilon_a \epsilon_c = B, \quad \epsilon_a \epsilon_b = C.$$

For a polygon configuration π (that is, a set of edges such that every vertex has even degree), a vertex of $\mathbb{H}_n$ is said to be of type ab if it is incident to two edges with types a and b (and similarly for ac and bc). Since each vertex in the polygon model has even degree, and $A = 0$, no vertex of $\mathbb{H}_n$ has type bc. Therefore, any polygon configuration with non-zero weight in $Z_n(P)$ is a disjoint union of cycles comprising ac-type and ab-type vertices. The vertices on such a cycle form consecutive pairs with the same type, and each such pair contributes weight either B^2 or C^2. It follows that $Z_n(P)$ is a sum of positive weights.

Let π' be a path between the midpoints of e to f that contributes a non-zero weight to $Z_{n,e\leftrightarrow f}$, and let h be the number of its a-type edges. Then π' contains exactly $2h$ vertices of $\mathbb{H}_n$, which appear in consecutive pairs with the same type (either ab or ac). The product of the weights of the vertices of π' is $B^{2v}C^{2(h-v)}$, where v is the number of consecutive pairs with type ac.

Since $D := B^2 + C^2 < 1$,

$$\begin{aligned}\langle \sigma_e \sigma_f \rangle_n &= \frac{Z_{n,e\leftrightarrow f}}{Z_n(P)} \\ &\leq \sum_{h=H}^{\infty} \sum_{v=0}^{h} \binom{h}{v} B^{2v} C^{2(h-v)} = \frac{D^H}{1-D},\end{aligned}$$

where H is the least h for which such π' exists. The claim follows.

Remark 4.2. *The conclusion (3.3) of Theorem 3.2 may be proved as follows subject to the more restrictive condition $a^2 < b^2 + c^2$. Under this condition, we have that $A, B, C < 0$. The graph $\mathbb{H}_n$ is bipartite with vertex-classes coloured black and white (see the discussion around Figure 2.2). We now reverse the signs of the spins of*

black vertices, thereby obtaining a ferromagnetic Ising model. It is easily checked that this is a high-temperature model (as in (4.17)), and it follows that $\langle \sigma_e \sigma_f \rangle \to 0$ *exponentially fast as* $|e - f| \to \infty$.

Remark 4.3. *A further proof of Theorem 3.2 is presented in Section 9. This proof is based on 'dimer' rather than 'Ising' methods, and may be extended to periodic 1-2 models which appear to be currently beyond the Kac–Ward techniques of* [29]. *See Section 10.*

5. Dimer representation of the 1-2 model

5.1. **The decorated dimer model.** Let $\mathbb{H}_{n,\Delta} = (V_{n,\Delta}, E_{n,\Delta})$ be the decorated toroidal graph derived from $\mathbb{H}_n$ and illustrated on the right of Figure 5.1. It was shown in [25] that there is a correspondence between 1-2 configurations on $\mathbb{H}_n$ and dimer configurations on $\mathbb{H}_{n,\Delta}$. This correspondence is summarized in the figure caption, and a more detailed description follows.

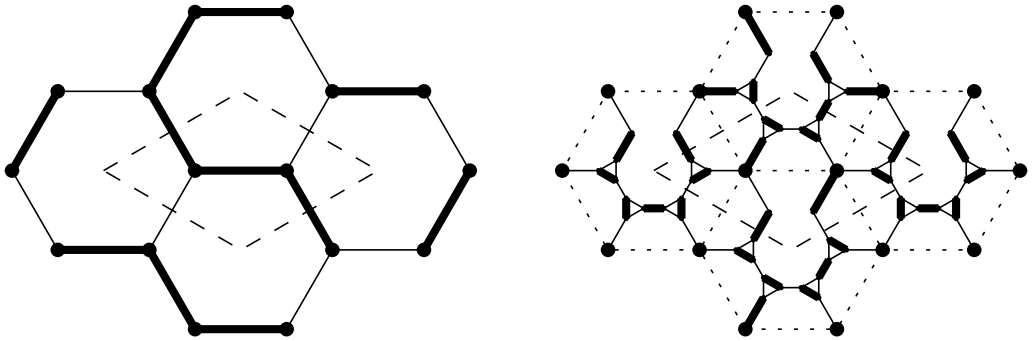

FIGURE 5.1. Part of a 1-2 configuration on $\mathbb{H}_n$, and the corresponding dimer (sub)configuration on $\mathbb{H}_{n,\Delta}$. When two edges with a common vertex of $\mathbb{H}_n$ have the same state in the 1-2 model, the corresponding 'bisector edge' is present in the dimer configuration. The states of the bisector edges determine the dimer configuration on the rest of $\mathbb{H}_{n,\Delta}$. The edges of $\mathbb{H}_{n,\Delta}$ are allocated weights consistently with the 1-2 weights of Figure 2.2. The central lozenge of the right-hand figure is expanded in Figure 5.3.

Let σ be a 1-2 configuration on $\mathbb{H}_n$, and let $v \in V_n$ ($\subseteq V_{n,\Delta}$). The vertex v has three incident edges in $\mathbb{H}_{n,\Delta}$, which are bisectors of the three angles of $\mathbb{H}_n$ at v. Such a *bisector edge* is present in the dimer configuration on $\mathbb{H}_{n,\Delta}$ if and only if the two edges of the corresponding angle have the same σ-state, that is, either both or neither are present. The states of the bisector edges determine the dimer configuration on

the entire $\mathbb{H}_{n,\Delta}$. Note that the 1-2 configurations σ and $-\sigma$ generate the same dimer configuration, denoted D_σ.

To the edges of $\mathbb{H}_{n,\Delta}$ we allocate weights as follows: edge $e = \langle i, j\rangle$ is allocated weight $w_{i,j}$ where

$$w_{i,j} = \begin{cases} a & \text{if } e \text{ is a horizontal bisector edge,} \\ b & \text{if } e \text{ is a NW bisector edge,} \\ c & \text{if } e \text{ is a NE bisector edge,} \\ 1 & \text{otherwise.} \end{cases} \tag{5.1}$$

The weight of a dimer configuration is the product of the weights of present edges.

To each 1-2 configuration σ on $\mathbb{H}_n$, there corresponds thus a unique dimer configuration on $\mathbb{H}_{n,\Delta}$. The converse is more complicated, and we preface the following discussion with the introduction of the planar graph $\mathbb{H}'_n$, derived from $\mathbb{H}_n$ by a process of 'unwrapping' the torus.

Let $\mathbb{H}'_n$ be the planar graph obtained from $\mathbb{H}_n$ by cutting through the two homology cycles γ_x and γ_y of the torus, as illustrated in Figure 5.2. That is, $\mathbb{H}'_n$ may be viewed as the set of edges that intersect the region marked in Figure 5.2 (in which $n = 4$ and the central edge is labelled $\langle u, v\rangle$). We may consider $\mathbb{H}'_n$ as a 'partial-graph' $\mathbb{H}'_n = (V_n, \widetilde{E}_n, H_n)$, where V_n is the vertex set, $\widetilde{E}_n$ is the 'internal' edge set, and H_n is the set of half-edges having one endpoint in V_n and one outside V_n. We write H_x^1 and H_x^2 (respectively, H_y^1, H_y^2) for the sets of half-edges that cross the upper left and lower right sides (respectively, upper right and lower left sides) of the diamond of Figure 5.2. Let $H_u = H_u^1 \cup H_u^2$ for $u = x, y$.

A 1-2 configuration on $\mathbb{H}'_n$ is a subset of edges and half-edges such that, for $v \in V_n$, the total number of edges and half-edges that are incident to v is either 1 or 2. It is explained in [25, p. 4] that dimer configurations on $\mathbb{H}_{n,\Delta}$ are in one-to-two correspondence to 1-2 configurations on $\mathbb{H}'_n$ satisfying any of the following (pairwise exclusive) conditions:

- (ss) for $e \in H_x \cup H_y$, the two corresponding half-edges $e^1 \in H_x^1 \cup H_y^1$, $e^2 \in H_x^2 \cup H_y^2$ have the same state (either both are present or neither is present);
- (os) for $e \in H_x$, the two corresponding half-edges $e^1 \in H_x^1$, $e^2 \in H_x^2$ have the opposite states (exactly one of them is present); for $e \in H_y$, the two corresponding half-edges $e^1 \in H_y^1$, $e^2 \in H_y^2$ have the same state;
- (so) for $e \in H_x$, the two corresponding half-edges $e^1 \in H_x^1$, $e^2 \in H_x^2$ have the same state; for $e \in H_y$, the two corresponding half-edges $e^1 \in H_y^1$, $e^2 \in H_y^2$ have the opposite states;
- (oo) for $e \in H_x \cup H_y$, the two corresponding half-edges $e^1 \in H_x^1 \cup H_y^1$, $e^2 \in H_x^2 \cup H_y^2$ have the opposite states.

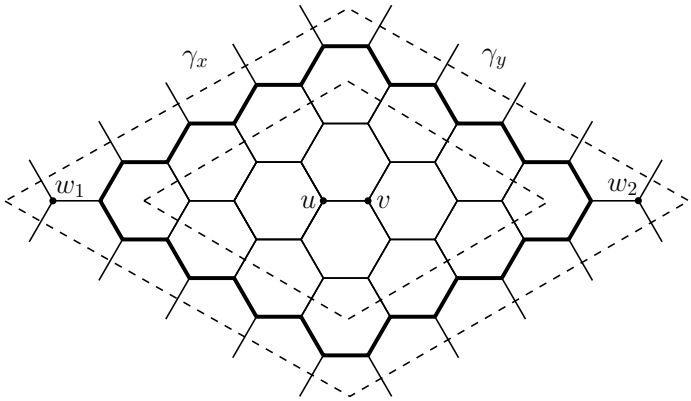

FIGURE 5.2. The $n \times n$ 'diamond' of $\mathbb{H}$, with $n = 4$. The region $\mathbb{H}'_n$ comprises all edges and half-edges that intersect the larger diamond. The annulus between the given boundaries comprises a cycle C_n (drawn above in bold), and two further edges incident with the w_i.

We refer to the above as the *mixed boundary condition* on $\mathbb{H}'_n$.

The above mixed boundary condition is more permissive than the periodic condition that gives rise to 1-2 configurations on the toroidal graph $\mathbb{H}_n$, although the difference turns out to be invisible in the infinite-volume limit (see Theorem 6.2).

5.2. **The spectral curve of the dimer model.** We turn now to the spectral curve of the above weighted dimer model on $\mathbb{H}_{n,\Delta}$. The reader is referred to [26] for relevant background, and to [25, Sect. 3] for further details of the following summary.

The fundamental domain of $\mathbb{H}_{n,\Delta}$ is the central lozenge of Figure 5.1, as expanded in Figure 5.3. The edges of $\mathbb{H}_{n,\Delta}$ are oriented as in the latter figure. It is easily checked that this orientation is 'clockwise odd', in the sense that any face of $\mathbb{H}_{n,\Delta}$, when traversed clockwise, contains an odd number of edges oriented in the corresponding direction. The fundamental domain has 16 vertices, and its weighted adjacency matrix (or 'Kasteleyn matrix') is the 16×16 matrix $\mathbf{B} = (b_{i,j})$ with

$$b_{i,j} = \begin{cases} w_{i,j} & \text{if } \langle i,j \rangle \text{ is oriented from } i \text{ to } j, \\ -w_{i,j} & \text{if } \langle i,j \rangle \text{ is oriented from } j \text{ to } i, \\ 0 & \text{if there is no edge between } i \text{ and } j, \end{cases}$$

where $w_{i,j}$ is given by (5.1). From $\mathbf{B}$ we obtain a *modified* adjacency (or 'Kasteleyn') matrix $\mathbf{B}(z,w)$ as follows.

We may consider the graph of Figure 5.3 as being embedded in a torus, that is, we identify the upper left boundary and the lower right boundary, and also the upper

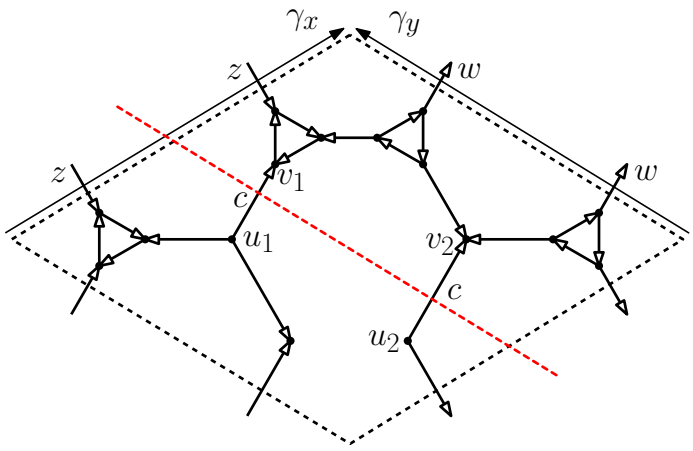

FIGURE 5.3. A single fundamental domain of the decorated graph $\mathbb{H}_{n,\Delta}$ obtained from the central lozenge of Figure 5.1. See that figure for an illustration of the relationship between this fundamental domain and the original hexagonal lattice $\mathbb{H}$. Note the homology cycles γ_x, γ_y of the torus, and also the two weight-c edges crossed by the central dashed line.

right boundary and the lower left boundary, as illustrated in the figure by dashed lines.

Let $w, z \in \mathbb{C}$ be non-zero. We orient each of the four boundaries of Figure 5.3 (denoted by dashed lines) from their lower endpoint to their upper endpoint. The 'left' and 'right' of an oriented portion of a boundary are as viewed by a person traversing in the given direction.

Each edge $\langle u, v \rangle$ crossing a boundary corresponds to two entries in the weighted adjacency matrix, indexed (u, v) and (v, u). If the edge starting from u and ending at v crosses an upper-left/lower-right boundary from left to right (respectively, from right to left), we modify the adjacency matrix by multiplying the entry (u, v) by z (respectively, z^{-1}). If the edge starting from u and ending at v crosses an upper-right/lower-left boundary from left to right (respectively, from right to left), in the modified adjacency matrix, we multiply the entry by w (respectively, w^{-1}). We modify the entry (v, u) in the same way. The ensuing matrix is denoted $\mathbf{B}(z, w)$, for a definitive expression of which, the reader is referred to [25, Sect. 3].

The *characteristic polynomial* is given (using Mathematica or otherwise) by

$$P(z, w) = \det \mathbf{B}(z, w) = f(a, b, c; w, z), \tag{5.2}$$

where

$$f(a,b,c;w,z) = a^4+b^4+c^4+6a^2b^2+6a^2c^2+6b^2c^2-2ab\left(z+\frac{1}{z}\right)\left(a^2+b^2-c^2\right) \\ -2ac\left(w+\frac{1}{w}\right)\left(a^2+c^2-b^2\right)-2bc\left(\frac{z}{w}+\frac{w}{z}\right)\left(b^2+c^2-a^2\right).$$

The *spectral curve* is the zero locus of the characteristic polynomial, that is, the set of roots of $P(z,w)=0$. It is proved in [25, Lemma 3.2] that the intersection of $P(z,w)=0$ with the unit torus $\mathbb{T}^2$ is either empty or a single real point $(1,1)$. Moreover, in the situation when $P(1,1)=0$, the zero $(1,1)$ has multiplicity 2. It will be important later to identify the conditions under which $P(1,1)=0$.

Proposition 5.1. *Let $a,b>0$ and $c\geq 0$.*

(a) *If any of the following hold,*

(i) $\sqrt{a}=\sqrt{b}+\sqrt{c}$, (ii) $\sqrt{b}=\sqrt{c}+\sqrt{a}$, (iii) $\sqrt{c}=\sqrt{a}+\sqrt{b}$,

the curve $P(z,w)=0$ intersects the unit torus $\mathbb{T}^2=\{(z,w):|z|=1,|w|=1\}$ at the unique point $(1,1)$.

(b) *If none of* (i)–(iii) *hold, the curve does not intersect the unit torus.*

Proof. The intersection of $P(z,w)=0$ with $\mathbb{T}^2$ can only be either empty or a single point $(1,1)$, by [25, Lemma 3.2]. Moreover, since

$$f(a,b,c;1,1)=(a^2+b^2+c^2-2ab-2bc-2ca)^2, \tag{5.3}$$

we have that $f(a,b,c;1,1)=0$ if and only if $\sqrt{a}\pm\sqrt{b}\pm\sqrt{c}=0$. □

We note for future use that

$$P(1,1)=f(a,b,c;1,1)=\tfrac{1}{4}\left[(A^2+B^2+C^2-1)(a+b+c)^2\right]^2, \tag{5.4}$$

where A, B, C are as in (4.2).

6. Infinite-volume limits

This paper is directed primarily at the asymptotic behaviour of the two-edge correlation function of the 1-2 model, rather than at the existence and multiplicity of infinite-volume measures. Partial results in the latter direction are reported in this section. In Section 6.1, the weak limit of the toroidal 1-2 measure is proved via a relationship with the dimer model on a decorated graph. In Section 6.2 we prove the non-uniqueness of Gibbs measures for the 'low temperature' 1-2 model. The existence of the infinite-volume free energy is proved in Section 6.3.

6.1. **Toroidal limit measure.** The 1-2 model may be studied via the dimer representation of Section 5. The dimer convergence theorem of [25] is as follows.

Theorem 6.1. [25, Prop. 3.3] *Consider the dimer measure $\delta_{n,\Delta}$ on $\mathbb{H}_{n,\Delta}$ with parameters $a, b, c > 0$. The limit measure $\delta_\Delta := \lim_{n\to\infty} \delta_{n,\Delta}$ exists and is translation-invariant and ergodic.*

Let μ_n^{mix} (respectively, μ_n) be the 1-2 probability measure on $\mathbb{H}'_n$ (respectively, on the toroidal $\mathbb{H}_n$) with parameters a, b, c and mixed boundary condition. By the results of [25] and the invariance of μ_n^{mix} under sign changes,

$$\mu_n^{\mathrm{mix}}(\sigma) = \mu_n^{\mathrm{mix}}(-\sigma) = \tfrac{1}{2}\delta_{n,\Delta}(D_\sigma), \tag{6.1}$$

where D_σ is the dimer configuration on $\mathbb{H}_{n,\Delta}$ corresponding to the 1-2 configuration σ on $\mathbb{H}'_n$. Since the topology of weak convergence may be given in terms of finite-dimensional cylinder events, the weak convergence $\delta_{n,\Delta} \to \delta_\Delta$ entails the weak convergence of μ_n^{mix} to some probability measure μ^{mix} on $\mathbb{H}$. By Theorem 6.1, μ^{mix} is translation-invariant. It is noted at [25, p. 17] that the ergodicity of δ_Δ does not imply that of μ^{mix}, and indeed there exist parameter values for which μ^{mix} is not ergodic, by the result of [25, Thm 4.9].

Theorem 6.2. *Let $a, b, c > 0$. The limit $\mu_\infty := \lim_{n\to\infty} \mu_n$ exists and satisfies $\mu_\infty = \mu^{\mathrm{mix}}$. In particular, for edges e, f of $\mathbb{H}$, the limit*

$$\langle \sigma_e \sigma_f \rangle := \lim_{n\to\infty} \langle \sigma_e \sigma_f \rangle_n \tag{6.2}$$

exists.

Proof. Let $\Omega_{n,\Delta}$ be the sample space of the dimer model on $\mathbb{H}_{n,\Delta}$. Let δ_n^{ev} be the probability measure of the dimer model on $\mathbb{H}_{n,\Delta}$ on the subspace $\Omega_{n,\Delta}^{\mathrm{ev}}$ of configurations with the property that, along each of the two zigzag paths of $\mathbb{H}$ that are neighbouring and parallel to γ_x and γ_y, there are an even number of present bisector edges.

As explained above (see also [25]), elements of $\Omega_{n,\Delta}$ correspond to 1-2 model configurations on $\mathbb{H}'_n$ with the mixed boundary condition, and of $\Omega_{n,\Delta}^{\mathrm{ev}}$ to 1-2 model configurations on the toroidal graph $\mathbb{H}_n$. We show next that

$$\delta_{n,\Delta}^{\mathrm{ev}} \to \delta_\Delta, \tag{6.3}$$

where $\delta_\Delta := \lim_{n\to\infty} \delta_{n,\Delta}$ is given in Theorem 6.1.

Let $Z_{n,\Delta}$ (respectively, $Z_{n,\Delta}^{\mathrm{ev}}$) be the partition function of $\Omega_{n,\Delta}$ (respectively, $\Omega_{n,\Delta}^{\mathrm{ev}}$), and let $K_n(z,w)$ be the modified Kasteleyn matrix of $\mathbb{H}_{n,\Delta}$ (see [25] and Section 5.2). As explained in [32, Sect. 4B], for $z, w \in \{-1, 1\}$, Pf $K_n(z,w)$ is a linear combination of partition functions of dimer configurations of four different classes, depending on

the parity of the present edges along the two zigag paths winding around the torus. In particular, by [32, Table 1, Sect. 4B], when n is even,

$$Z^{\mathrm{ev}}_{n,\Delta} = \tfrac{1}{4}\Big[\mathrm{Pf}\, K_n(1,1) + \mathrm{Pf}\, K_n(-1,1) + \mathrm{Pf}\, K_n(1,-1) + \mathrm{Pf}\, K_n(-1,-1)\Big].$$

Let $e_i = \langle u_i, v_i\rangle$, $1 \le i \le k$, be edges of $\mathbb{H}_{n,\Delta}$, and let $M(e_1,\dots,e_k)$ be the event that every e_i is occupied by a dimer. Let $w_i > 0$ be the edge weight of e_i. Then

$$\delta^{\mathrm{ev}}_n(M(e_1,\dots,e_k)) = \prod_{i=1}^k w_{e_i} \left| \frac{\mathrm{Pf}\, \widehat{K}_n(1,1) + \mathrm{Pf}\, \widehat{K}_n(-1,1) + \mathrm{Pf}\, \widehat{K}_n(1,-1) + \mathrm{Pf}\, \widehat{K}_n(-1,-1)}{\mathrm{Pf}\, K_n(1,1) + \mathrm{Pf}\, K_n(-1,1) + \mathrm{Pf}\, K_n(1,-1) + \mathrm{Pf}\, K_n(-1,-1)} \right|,$$

where $\widehat{K}_n$ is the submatrix of K_n obtained by removing rows and columns indexed by $u_1, v_1, \dots, u_k, v_k$. As in [3, Thm 4],

(6.4)

$$\delta_{n,\Delta}(M(e_1,\dots,e_k)) = \prod_{i=1}^k w_{e_i} \left| \frac{-\mathrm{Pf}\, \widehat{K}_n(1,1) + \mathrm{Pf}\, \widehat{K}_n(-1,1) + \mathrm{Pf}\, \widehat{K}_n(1,-1) + \mathrm{Pf}\, \widehat{K}_n(-1,-1)}{-\mathrm{Pf}\, K_n(1,1) + \mathrm{Pf}\, K_n(-1,1) + \mathrm{Pf}\, K_n(1,-1) + \mathrm{Pf}\, K_n(-1,-1)} \right|.$$

As in the proof of [3, Thm 6], $\delta^{\mathrm{ev}}_{n,\Delta}(M(e_1,\dots,e_k))$ and $\delta_{n,\Delta}(M(e_1,\dots,e_k))$ converge as $n \to \infty$ to the same complex integral. Since the events $M(e_1,\dots,e_k)$ generate the product σ-field, we deduce (6.3).

Finally, we deduce the claim of the theorem. An *even* (respectively, *odd*) *correlation function* is an expectation of the form $\langle \sigma_A \rangle$, with $\sigma_A = \prod_{e\in A} \sigma_e$ where A is a finite set of edges of $\mathbb{H}$ with even (respectively, odd) cardinality. In order that $\mu_n \to \mu^{\mathrm{mix}}$, it suffices that the correlation functions of μ_n and μ^{mix}_n have the same limit. By invariance under sign change, the odd correlation functions equal 0.

The relationship between a 1-2 measure μ and the corresponding dimer measure δ is as follows. Let $e_1,\dots,e_k$ be bisector edges of $\mathbb{H}_{n,\Delta}$, and let $S(e_1,\dots,e_k)$ be the event that every e_i separates two edges of $\mathbb{H}_n$ with the same 1-2 state. Using the correspondence between 1-2 and dimer configurations,

$$\mu(S(e_1,\dots,e_k)) = \delta(M(e_1,\dots,e_k)).$$

Let $k \ge 1$, let $e_1, e_2, \dots, e_{2k}$ be distinct edges of $\mathbb{H}_n$, and write $\sigma_i = \sigma_{e_i}$. Then

$$\langle \sigma_1 \cdots \sigma_{2k} \rangle_\mu = 1 - 2\mu(\sigma_1 \cdots \sigma_{2k} = -1). \tag{6.5}$$

For $i = 2, 3, \dots, 2k$, let π_i be a self-avoiding path between the midpoints of e_1 and e_i comprising edges of $\mathbb{H}_n$ and two half-edges, and let $\mathcal{A}_i$ be the event that the number of *absent* bisector edges encountered along π_i is odd. As we move along π_i in the

1-2 model, the edge-state changes at a given vertex if and only if the corresponding bisector edge is absent. Therefore, $\sigma_1\sigma_i = -1$ if and only if $\mathcal{A}_i$ occurs, so that

$$\langle \sigma_e \sigma_f \rangle_\mu = \mu(\overline{\mathcal{A}}_i) - \mu(\mathcal{A}_i). \tag{6.6}$$

Let $\mathcal{A}$ be the event that the set $I = \{i : \mathcal{A}_i \text{ occurs}\}$ has odd cardinality. Since $I = \{i : \sigma_1 \neq \sigma_i\}$, we have that

$$\mu(\sigma_1 \cdots \sigma_{2k} = -1) = \delta(\mathcal{A}). \tag{6.7}$$

We return to the measures μ_n and μ_n^{mix}. By (6.3)–(6.7), the even correlation functions of μ_n and μ_n^{mix} are convergent as $n \to \infty$, with equal limits. It follows that $\mu_n \to \mu_\infty$ where $\mu_\infty = \mu^{\text{mix}}$. □

6.2. **Non-uniqueness of Gibbs measures.** We show the existence of at least two Gibbs measures (that is, 'phase coexistence') for the 'low temperature' 1-2 model on $\mathbb{H}$. Let Σ be the set of 1-2 configurations on the infinite lattice $\mathbb{H}$, and let $\mathcal{G} = \mathcal{G}(a, b, c)$ be the set of probability measures on Σ that satisfy the appropriate DLR condition. (We omit the details of DLR measures here, instead referring the reader to the related discussions of [2, Sect. 2.3] and [14, Sect. 4.4].) Since Σ is compact, by Prohorov's theorem [1, Sect. 1.5], every sequence of probability measures on Σ has a convergent subsequence. It may be shown that any weak limit of finite-volume 1-2 measures lies in $\mathcal{G}$, and hence $\mathcal{G} \neq \varnothing$.

Theorem 6.3. *Let $a \geq b > 0$. For almost every c satisfying either $0 < \sqrt{c} < \sqrt{a} - \sqrt{b}$ or $\sqrt{c} > \sqrt{a} + \sqrt{b}$, we have that $|\mathcal{G}| \geq 2$.*

Proof. This proof is inspired by that of [2, Thm 6.2], and it makes use of Theorem 3.1, the proof of which has been deferred to Section 7. Let e be a given horizontal edge of $\mathbb{H}_n$, and let f_m be an edge satisfying (3.1) such that $\pi(e, f_m)$ has length m. By Theorem 3.1(b) and translation invariance, for almost every c satisfying the given inequalities, there exists $\alpha > 0$ such that

$$\lim_{m\to\infty} \langle \sigma_e \sigma_{f_m} \rangle^2 = \alpha^2, \tag{6.8}$$

where $\langle \sigma_e \sigma_f \rangle$ is the limiting two-edge correlation as $n \to \infty$ (see Theorem 6.2). It suffices to show that, subject to (6.8), $|\mathcal{G}| \geq 2$.

By (6.8), there exists a subsequence $(m_k : k \geq 1)$ along which $\langle \sigma_e \sigma_{f_{m_k}} \rangle$ converges to either α or $-\alpha$. Assume the first; the proof is essentially the same in the second case. For simplicity of notation, we shall assume that

$$\lim_{m\to\infty} \langle \sigma_e \sigma_{f_m} \rangle = \alpha.$$

By the invariance of μ_∞ under sign change of the configuration,

$$\lim_{m\to\infty} \mu_\infty(\sigma_e = 1 \mid \sigma_{f_m} = 1) = \tfrac{1}{2}(1+\alpha),$$
$$\lim_{m\to\infty} \mu_\infty(\sigma_e = 1 \mid \sigma_{f_m} = -1) = \tfrac{1}{2}(1-\alpha).$$

Find M such that

$$\begin{aligned}\mu_\infty(\sigma_e = 1 \mid \sigma_{f_m} = -1) &< \tfrac{1}{2}(1 - \tfrac{1}{2}\alpha)\\ &< \tfrac{1}{2}(1+\tfrac{1}{2}\alpha) < \mu_\infty(\sigma_e = 1 \mid \sigma_{f_m} = 1), \qquad m \ge M.\end{aligned}$$

We may find an increasing subsequence $(r_m : m \ge M)$ such that

$$\begin{aligned}\mu_{r_m}(\sigma_e = 1 \mid \sigma_{f_m} = -1) &< \tfrac{1}{2}(1 - \tfrac{1}{3}\alpha)\\ &< \tfrac{1}{2}(1+\tfrac{1}{3}\alpha) < \mu_{r_m}(\sigma_e = 1 \mid \sigma_{f_m} = 1), \qquad m \ge M.\end{aligned}$$

Let μ^+ (respectively, μ^-) be a subsequential limit of $\mu_{r_m}(\cdot \mid \sigma_{f_m} = 1)$ (respectively, $\mu_{r_m}(\cdot \mid \sigma_{f_m} = -1)$), so that

$$\mu^+(\sigma_e = 1) > \mu^-(\sigma_e = 1).$$

In particular, $\mu^+ \ne \mu^-$. Since $|e - f_m| \to \infty$ as $m \to \infty$, the measures $\mu^\pm$ satisfy the DLR condition, and therefore they lie in $\mathcal{G}$. □

6.3. **Free energy.** A *boundary condition* $\mathcal{B}_n$ is a configuration on the half-edges H_n of the planar graph $\mathbb{H}'_n = (V_n, \widetilde{E}_n, H_n)$, in the notation of Section 6.1. Let $Z_n(a,b,c,\mathcal{B}_n)$ be the partition function of the 1-2 model on $\mathbb{H}'_n$ with parameters a, b, c and boundary condition $\mathcal{B}_n$ (as in (4.1), say). The free energy, for given a, b, c and boundary conditions $(\mathcal{B}_n : n \ge 1)$, is defined to be

$$\mathcal{F}(a,b,c,(\mathcal{B}_n)) := \lim_{n\to\infty} \frac{1}{|V_n|} \log Z_n(a,b,c,\mathcal{B}_n), \tag{6.9}$$

whenever the limit exists.

Proposition 6.4. *Let $(a,b,c) \ne (0,0,0)$. The free energy of (6.9) exists and is independent of the choice of boundary conditions $(\mathcal{B}_n)$. Moreover, up to a smooth additive constant, it satisfies*

$$\mathcal{F}(a,b,c) = \frac{1}{4\pi^2} \iint_{[0,2\pi]^2} \log P(e^{i\theta}, e^{i\phi})\, d\theta\, d\phi, \tag{6.10}$$

where P is given in (5.2).

Proof. The correspondence between 1-2 model configurations on $\mathbb{H}'_n$ (with the mixed boundary condition) and dimer configurations on $\mathbb{H}_{n,\Delta}$ was explained in Section 6.1. It follows that the free energy of that 1-2 model is the same as that of the corresponding dimer model. The expression (6.10) follows for that case from a general

argument used to compute the free energy of this dimer model, given that either the spectral curve does not intersect the unit torus, or the intersection is a unique real point of multiplicity 2. See Proposition 5.1 and also [22, Thm 3.5] and [3, Thm 1].

Next we prove that the free energy of (6.9) is independent of the choice of $(\mathcal{B}_n)$. To this end, we consider the boxes $\mathbb{H}'_n$ and $\mathbb{H}'_{n-2}$ illustrated in Figure 5.2. We claim that, for any boundary condition on $\mathbb{H}'_n$ (that is, any present/absent configuration on H_n) and any 1-2 model configuration on $\mathbb{H}'_{n-2}$ (so that the edge-states on $\widetilde{E}_{n-2} \cup H_{n-2}$ are given), there exists a configuration on $\widetilde{E}_n \setminus (\widetilde{E}_{n-2} \cup H_{n-2})$ such that the composite configuration is a 1-2 configuration on $\mathbb{H}'_n$.

This claim is shown as follows. Consider a given boundary condition on H_n and a 1-2 configuration on $\mathbb{H}'_{n-2}$. The vertex-set $V_n \setminus V_{n-2}$ forms a cycle C_n with even length, together with two further vertices w_1, w_2 at the left and right corners, see Figure 5.2. From C_n we select a perfect matching. By considering the various possibilities, we may see that it is always possible to allocate states to the two edges between C_n and the w_i in such a way that, in the resulting composite configuration, each w_i has degree either 1 or 2.

Let $\mathcal{B}_n^0$ be the *free boundary condition*, under which no half-edge is present. We have that

$$\left|\log Z_n(a,b,c,\mathcal{B}_n) - \log Z_{n-2}(a,b,c,\mathcal{B}_{n-2}^0)\right| \le |V_n \setminus V_{n-2}|K,$$

for some $K = K(a,b,c) > 0$ and all $\mathcal{B}_n$. Divide by $|V_n|$ and let $n \to \infty$ to obtain the claim. The theorem follows on noting that the number of boundary configurations is $2^{|H_n|}$, and $|H_n|/|V_n| \to 0$ as $n \to \infty$. □

7. Proof of Theorem 3.1(a, b, c)

The basic structure of the proof is as follows. As in Section 5, the 1-2 model may be represented as a dimer model on a certain decorated graph $\mathbb{H}_{n,\Delta}$ derived from $\mathbb{H}_n$. Subject to condition (3.1), the two-edge correlation $\langle \sigma_e \sigma_f \rangle_n$ of the 1-2 model may be represented in terms of certain cylinder probabilities of the dimer model. Using the theory of dimers, these probabilities may be expressed in terms of ratios of Pfaffians of block Toeplitz matrices, and a similar representation follows for the infinite-volume two-edge correlation $\langle \sigma_e \sigma_f \rangle$. By Widom's theorem [37, 38], the limit $\Lambda(a,b,c) := \lim_{|e-f|\to\infty} \langle \sigma_e \sigma_f \rangle^2$ exists, and furthermore Λ is analytic except when the spectral curve intersects the unit torus. This identifies the phases of the 1-2 model, and they may be identified as sub/supercritical via the extreme values of (3.2).

We assume henceforth that the edges e, f of $\mathbb{H}$ satisfy the following condition:

(7.1) e and f are midpoints of two NW edges such that there exists a path $\pi = \pi(e,f)$ in $A\mathbb{H}_n$ from e to f using only horizontal and NW half-edges.

See Figure 7.1. The principal step in the proof is the following.

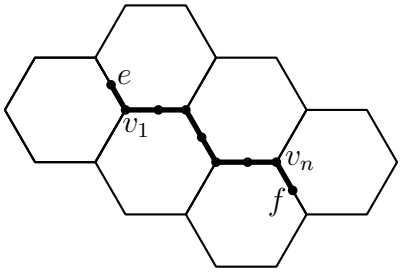

FIGURE 7.1. A path π comprising horizontal and NW mid-edges, connecting the midpoints of two NW edges e and f.

Theorem 7.1. *Let e, f be two edges satisfying (7.1), and let $a \geq b \geq 0$. The limit $\Lambda(a,b,c) := \lim_{|e-f|\to\infty} \langle \sigma_e \sigma_f \rangle^2$ is complex analytic in $c \geq 0$ except when $\sqrt{c} = \sqrt{a} - \sqrt{b}$ and $\sqrt{c} = \sqrt{a} + \sqrt{b}$.*

Proof of Theorem 3.1. Part (a) holds by Theorem 6.2. Let $a \geq b > 0$. By Theorem 7.1, the function $\Lambda_3(\cdot) := \Lambda(a,b,\cdot)$ is complex analytic on each of the intervals

$$C_1 = \big[0, (\sqrt{a} - \sqrt{b})^2\big),$$
$$C_2 = \big((\sqrt{a} - \sqrt{b})^2, (\sqrt{a} + \sqrt{b})^2\big),$$
$$C_3 = \big((\sqrt{a} + \sqrt{b})^2, \infty\big).$$

(That is to say, for $c \in C_i$ considered as a line in the complex plane, Λ_3 is analytic on some open neighbourhood of c.) By Remark 4.2, $\Lambda_3(c) = 0$ when $c \in S := (\sqrt{a^2 - b^2}, \sqrt{a^2 + b^2})$. Since $S \subseteq C_2$ and Λ_3 is analytic on C_2, the claim of part (c) follows. (The claim is trivial if $a = b$.)

We turn to part (b). Consider first the interval C_1, and assume $a > b$. Since non-trivial analytic functions have only isolated zeros, it follows that: either $\Lambda_3 \equiv 0$ on C_1, or Λ_3 is non-zero except possibly on a set of isolated points of C_1. By (3.2), $\Lambda_3(0) = 1$, whence the latter holds.

By (3.2), $\langle \sigma_e \sigma_f \rangle = 1$ when $a = b = 0$ and $c = 1$. Since Λ_3 is analytic (and hence continuous) on C_3, there exists $\alpha > 0$ such that $\Lambda(a,b,c) \geq \alpha$ in a small (real) neighbourhood of $(0,0,1)$. Since Λ depends only on the ratios $a : b : c$ (cf. (2.5)), we deduce that, for fixed $a, b > 0$ and sufficiently large c, we have $\Lambda_3(c) \geq \alpha > 0$. By Theorem 7.1, Λ_3 is analytic on C_3, and the claim holds as above. □

The remainder of the section is devoted to the proof of Theorem 7.1. We shall develop the notation and arguments of Section 6.1. Let μ_n^{mix} be the 1-2 measure on $\mathbb{H}'_n$ with the mixed boundary condition of Section 6.1, and let $\mu^{\mathrm{mix}} := \lim_{n\to\infty} \mu_n^{\mathrm{mix}}$,

as after Theorem 6.1. By Theorem 6.2, the 1-2 measure μ_n on $\mathbb{H}_n$ satisfies $\mu_n \to \mu_\infty = \mu^{\text{mix}}$ as $n \to \infty$.

Let e, f be edges of the hexagonal lattice $\mathbb{H}$ satisfying (7.1). Let the path π of (7.1) traverse a total of $2k-1$ edges and two half-edges, so that π passes $2k$ bisector edges of the infinite decorated graph $\mathbb{H}_\Delta$. We denote this set of bisector edges by

$$B = \{b_i = \langle u_i, v_i\rangle : i = 1, 2, \dots, k\}, \tag{7.2}$$

where $v_i \in \pi$.

Our target is to represent $\langle \sigma_e \sigma_f \rangle$ as the Pfaffian of a truncated block Toeplitz matrix, as inspired by [19, Sect. 4.7]. A principal difference between [19] and the current work is that, whereas bipartite graphs are considered there and the determinants of weighted adjacency matrices are computed, in the current setting the graph is non-bipartite and we will compute Pfaffians.

To $\mathbb{H}_\Delta$ we assign a clockwise odd orientation as in Figure 5.3: the figure shows a clockwise odd orientation of $\mathbb{H}_{1,\Delta}$, embedded in a 1×1 torus, that lifts to a clockwise odd orientation of $\mathbb{H}_\Delta$. As in (5.1), a horizontal (respectively, NW, NE) bisector edge of $\mathbb{H}_\Delta$ is assigned weight a (respectively, b, c), and all the other edges are assigned weight 1. The bisector edges $g_i = \langle u_i, v_i\rangle$ are oriented in such a way that each g_i is oriented from u_i to v_i in this clockwise-odd orientation.

Let K_n be the Kasteleyn matrix of $\mathbb{H}_{n,\Delta}$ (as in Section 5.2 and [25]), and let $|v|$ denote the index of the row and column of K_n corresponding to the vertex v. Assume that $|v_i| = |u_i| + 1$ for $1 \le i \le 2k$, and furthermore that

$$|u_1| < |v_1| < |u_2| < |v_2| < \cdots < |u_k| < |v_k|. \tag{7.3}$$

Let K^{-1} be the infinite matrix whose entries are the limits of the entries of K_n^{-1} as $n \to \infty$. The existence of K^{-1} may be proved by an explicit diagonalization of K_n using periodicity, as in [8, Sect. 7] and [24].

We now construct the modified Kasteleyn matrix $K_1(z, w)$ of $\mathbb{H}_{1,\Delta}$ by multiplying the corresponding entries in its Kasteleyn matrix by z or z^{-1} (respectively, w or w^{-1}), according to the manner in which the edge crosses one of the two homology cycles γ_x, γ_y indicated in Figure 5.3. As remarked in Section 5.2, the characteristic polynomial $P(z, w) = \det K_1(z, w)$ is the function $f(a, b, c; w, z)$ of (5.2), see also [25, Lemma 9]. The intersection of the spectral curve $P(z, w) = 0$ and the unit torus $\mathbb{T}^2$ is given by Proposition 5.1.

Consider the toroidal graph $\mathbb{H}_{n,\Delta}$. Let γ_x, γ_y be homology cycles of the torus, which for definiteness we take to be shortest cycles composed of unions of boundary segments of fundamental domains as in Figure 5.3. Let $K_n(z, w)$ be the modified Kasteleyn matrix of $\mathbb{H}_{n,\Delta}$.

For $I \subseteq \{1, 2, \dots, 2k\}$, let M_I be the event that every b_i with $i \in I$ is present in the dimer configuration. Assume n is sufficiently large that

$$\text{for } 1 \le i \le 2k, \quad \text{the edge } b_i \text{ intersects neither } \gamma_x \text{ nor } \gamma_y. \tag{7.4}$$

For n even, as in (6.4),

(7.5)

$$\begin{aligned}\mu_\infty(M_I) &= \lim_{n\to\infty} \mu_n(M_I)\\ &= \lim_{n\to\infty} J_I \frac{-\mathrm{Pf}\,\widehat{K}_{n,I}(1,1) + \mathrm{Pf}\,\widehat{K}_{n,I}(1,-1) + \mathrm{Pf}\,\widehat{K}_{n,I}(-1,1) + \mathrm{Pf}\,\widehat{K}_{n,I}(-1,-1)}{-\mathrm{Pf}\,K_n(1,1) + \mathrm{Pf}\,K_n(1,-1) + \mathrm{Pf}\,K_n(-1,1) + \mathrm{Pf}\,K_n(-1,-1)},\end{aligned}$$

where

$$J_I = \prod_{i\in I} [K_n]_{u_i,v_i}, \tag{7.6}$$

and $\widehat{A}_I$ denotes the submatrix of the matrix A after deletion of rows and columns corresponding to $\{u_i, v_i : i \in I\}$ (see [25, Thm 0.1]). Note that $\mu_\infty(M_\varnothing) = 1$.

The limit of (7.5) can be viewed as follows. Each monomial in the expansion of $\mathrm{Pf}\,K_n(z,w)$, $z, w \in \{-1, 1\}$, corresponds to the product of edge-weights of a dimer configuration, but may have negative sign; the linear combination of $\mathrm{Pf}\,K_n(1,1)$, $\mathrm{Pf}\,K_n(1,-1)$, $\mathrm{Pf}\,K_n(-1,1)$, and $\mathrm{Pf}\,K_n(-1,-1)$ is chosen in such a way that the products of edge-weights of different dimer configurations correspond to monomials of the same sign. The numerator of (7.5) is the sum over dimer configurations containing every b_i, $i \in I$; this can be computed by the corresponding sum of monomials in the expansion of the denominator. Under (7.4), $[K_n]_{u_i,v_i} := [K_n(z,w)]_{u_i,v_i}$ is independent of $z, w \in \{-1, 1\}$. Since each b_i is oriented from u_i to v_i, we have that $[K_n]_{u_i,v_i} = c$, whence $J_I = c^{|I|}$.

Lemma 7.2. *Let A be a $2m \times 2m$ invertible, anti-symmetric matrix, and let $L \subseteq \{1, 2, \dots, 2m\}$ be a nonempty even subset. Let $\widehat{A}_L$ be the submatrix of A obtained by deleting the rows and columns indexed by elements in L, and let A_L^{-1} be the submatrix of A^{-1} with rows and columns indexed by elements in L. Then*

$$(-1)^{S(L)}\mathrm{Pf}\,\widehat{A}_L = \mathrm{Pf}\,(A)\mathrm{Pf}\,(A_L^{-1}), \quad \text{where } S(L) = \sum_{l\in L} l.$$

Proof. See the Appendix in Section 11. □

The conclusion of Lemma 7.2 holds also when $L = \varnothing$, subject to the convention that $\mathrm{Pf}\,(A_\varnothing^{-1}) = 1$.

Returning to (7.5), take $L = \{|u_i|, |v_i| : i \in I\}$, so that $(-1)^{S(L)} = (-1)^{|I|}$. When the spectral curve does not intersect the unit torus $\mathbb{T}^2$, by Lemma 7.2,

$$\begin{aligned}\lim_{n\to\infty} \frac{\operatorname{Pf} \widehat{K}_{n,I}(z,w)}{\operatorname{Pf} K_n(z,w)} &= \lim_{n\to\infty} (-1)^{|I|} \operatorname{Pf} K_{n,I}^{-1}(z,w) \\ &= (-1)^{|I|} \operatorname{Pf} K_I^{-1},\end{aligned}$$

where the limit is independent of $z, w \in \{-1, 1\}$; see [24, Lemma 4.8] for a proof of the existence of the limits of the entries of K_n^{-1}. By (7.5)–(7.6),

$$\mu_\infty(M_I) = (-c)^{|I|} \operatorname{Pf} K_I^{-1}. \tag{7.7}$$

We shall make use of the following elementary lemma, the proof of which is omitted.

Lemma 7.3. *Let S be a random subset of the finite nonempty set B. The probability generating function (pgf) $G(x) = \mathbb{E}(x^{|S|})$ satisfies*

$$G(1+\lambda) = \sum_{I \subseteq B} \lambda^{|I|} \mathbb{P}(S \supseteq I), \qquad \lambda \in \mathbb{R}.$$

Let B be the set of bisector edges along π (see (7.2)), and let S be the subset of such edges that are present in the dimer configuration. By (6.6),

$$\langle \sigma_e \sigma_f \rangle = G(-1),$$

where G is the pgf of $|S|$ under the measure μ_∞. By (7.7) and Lemma 7.3,

$$\langle \sigma_e \sigma_f \rangle = \sum_{I \subseteq B} (-2)^{|I|} \mu_\infty(M_I) = \sum_{I \subseteq B} (2c)^{|I|} \operatorname{Pf} K_I^{-1}. \tag{7.8}$$

This may be recognized as the Pfaffian of a certain matrix defined as follows.

Let $Y_1(\lambda)$ be the 2×2 matrix

$$Y_1(\lambda) = \begin{pmatrix} 0 & \lambda \\ -\lambda & 0 \end{pmatrix},$$

and let $Y_{2k}(\lambda)$ be the $4k \times 4k$ block diagonal matrix with diagonal 2×2 blocks equal to $Y_1(\lambda)$. More precisely, $Y_{2k}(\lambda)$ has rows and columns indexed $u_1, v_1, u_2, v_2, \ldots, u_{2k}, v_{2k}$, and

$$Y_{2k}(\lambda) = \begin{pmatrix} Y_1(\lambda) & 0 & \cdots & 0 \\ 0 & Y_1(\lambda) & \cdots & 0 \\ \vdots & \vdots & \ddots & \vdots \\ 0 & 0 & \cdots & Y_1(\lambda) \end{pmatrix}.$$

Lemma 7.4. *We have that*

$$\langle \sigma_e \sigma_f \rangle = \operatorname{Pf} [Y_{2k}(1) + 2c K_{V_\pi}^{-1}], \tag{7.9}$$

where $V_\pi = \{u_1, v_1, u_2, v_2, \ldots, u_{2k}, v_{2k}\}$.

Proof. It suffices by (7.8) that

$$\operatorname{Pf}[Y_{2k}(1)+A] = \sum_{I\subseteq B} \operatorname{Pf} A_I, \tag{7.10}$$

where $A = (a_{i,j})$ is a $4k \times 4k$ anti-symmetric matrix with consecutive pairs of rows/columns indexed by the set $B = \{1, 2, \dots, 2k\}$, and A_I is the submatrix of A with pairs of rows and columns indexed by $I \subseteq B$.

Let $G = (V, E)$ be the complete graph with vertex-set $V = \{1, 2, \dots, 4k\}$, and recall that

$$\operatorname{Pf} A = \sum_{\mu\in\Pi} \operatorname{sgn}(\pi_\mu) \prod_{\substack{(i,j)\in\mu\\ i<j}} a_{i,j}, \tag{7.11}$$

(see [17, 35]), where Π is the set of perfect matchings of G, and the permutation $\pi_\mu \in S_{4k}$ is given by

$$\pi_\mu = \begin{pmatrix} 1 & 2 & 3 & 4 & \cdots & 4k-1 & 4k \\ i_i & j_1 & i_2 & j_2 & \cdots & i_{2k} & j_{2k} \end{pmatrix} \tag{7.12}$$

where $\mu = \{(i_r, j_r) : 1 \le r \le 2k\}$, $i_1 < i_2 < \cdots < i_{2k}$, and $i_r < j_r$.

By (7.11),

$$\begin{aligned} \operatorname{Pf}[Y_{2k}(1)+A] &= \sum_{\mu\in\Pi} \operatorname{sgn}(\pi_\mu) \prod_{\substack{(i,j)\in\mu\\ i<j}} [Y_{2k}(1)+A]_{i,j} \\ &= \sum_{K\subseteq V} \left(\sum_{\mu\in\Pi} \operatorname{sgn}(\pi_\mu) \prod_{\substack{(i,j)\in\mu\\ i\in K,\ i<j}} [Y_{2k}(1)]_{i,j} \prod_{\substack{(i,j)\in\mu\\ i\notin K,\ i<j}} a_{i,j} \right). \end{aligned} \tag{7.13}$$

The penultimate product is 0 unless every $i \in K$ is odd and satisfies $(i, i+1) \in \mu$. Therefore, with $J = \frac{1}{2}(K+1) \subseteq B$,

$$\begin{aligned} \operatorname{Pf}[Y_{2k}(1)+A] &= \sum_{J\subseteq B} \left(\sum_{\mu\in\Pi} \operatorname{sgn}(\pi_\mu) \prod_{\substack{(i,j)\in\mu,\ i<j\\ i,j\notin(2J-1)\cup(2J)}} a_{i,j} \right) \\ &= \sum_{J\subseteq B} \operatorname{Pf} A_{B\setminus J}, \end{aligned}$$

as required for (7.10). □

Now, $Y_{2k}(1) + 2cK_{V_\pi}^{-1}$ is a truncated block Toeplitz matrix each block of which has size 4×4. We propose to use Widom's formula (see Theorem 7.7) to study the limit

of its determinant as $k \to \infty$. In this limit, the matrix becomes an infinite block Toeplitz matrix $T(\psi)$ with symbol given by

$$\psi(z) = \frac{1}{2\pi} \int_0^{2\pi} \phi(z, e^{i\theta})\, d\theta \tag{7.14}$$

where

$$\phi(z, e^{i\theta}) = Y_2(1) + 2cK_1^{-1}(z, e^{i\theta})_{(1:4)}, \tag{7.15}$$

and $A_{(1:4)}$ denotes the 4×4 submatrix of the matrix A with rows and columns indexed by u_1, v_1, u_2, v_2 as in Figure 5.3. This follows by the explicit calculation

$$[K^{-1}]_{u,v} = \frac{1}{4\pi^2} \int_0^{2\pi} \int_0^{2\pi} e^{ik\phi} [K_1^{-1}(e^{i\theta}, e^{i\phi})]_{u,v'}\, d\theta\, d\phi, \qquad u, v \in V_\pi, \tag{7.16}$$

where v' is the translation of v to the same fundamental domain as u, and k is the number of fundamental domains traversed in moving from v' to v, with sign depending on the direction of the move. When $k \neq 0$, (7.16) is the kth Fourier coefficient of the symbol (7.14). See [24, Sect. 4] for a similar computation.

Lemma 7.5. *Let $z \in \mathbb{C}$ with $|z| = 1$. When the spectral curve does not intersect the unit torus $\mathbb{T}^2$, we have that* $\det \psi(z) = 1$.

Proof. Let $\mathbb{H}_{m,n,\Delta}$ be the toroidal graph comprising $m \times n$ fundamental domains (a fundamental domain is drawn in Figure 5.3). We can think of $\mathbb{H}_{m,n,\Delta}$ as the quotient graph of $\mathbb{H}_\Delta$ under the action of $m\mathbb{Z} \times n\mathbb{Z}$. To $\mathbb{H}_{m,n,\Delta}$ we allocate the clockwise-odd orientation of Figure 5.3.

Let $K_{m,n}(z, w)$ be the corresponding modified Kasteleyn matrix. Assume the cycle γ_x (respectively, γ_y) crosses $2n$ (respectively, $2m$) edges, whose weights are multiplied by z or z^{-1} (respectively, w or w^{-1}), depending on their orientations. Note that $K_{1,1} = K_1$.

The toroidal graph $\mathbb{H}_{1,n,\Delta}$ is a line of n copies of the graph of Figure 5.3, aligned parallel to γ_x. It contains $2n$ (bisector) edges with weight c, of which we select two, denoted e_1, e_2, lying in the same fundamental domain. Let $\mathbb{H}^*_{1,n,\Delta}$ be the oriented graph obtained from $\mathbb{H}_{1,n,\Delta}$ by reversing the orientations of e_1 and e_2, and let $K^*_{1,n}(z, w)$ be the modified Kasteleyn matrix of $\mathbb{H}^*_{1,n,\Delta}$.

Let $X(\lambda)$ be the $4n \times 4n$ matrix

$$X(\lambda) = \begin{pmatrix} Y_1(\lambda) & 0 & 0 \\ 0 & Y_1(\lambda) & 0 \\ 0 & 0 & 0 \end{pmatrix}.$$

Since e_1 and e_2 have weight c,

$$\begin{aligned}\frac{\det K^*_{1,n}(z,w)}{\det K_{1,n}(z,w)} &= \frac{\det[K^*_{1,n}(z,w) - K_{1,n}(z,w) + K_{1,n}(z,w)]}{\det K_{1,n}(z,w)} \\ &= \frac{\det\left[X(-2c) + K_{1,n}(z,w)\right]}{\det K_{1,n}(z,w)} \\ &= \det\left[X(-2c)K^{-1}_{1,n}(z,w) + I\right] \\ &= \det\left[Y_2(-2c)K^{-1}_{1,n}(z,w)_{(1:4)} + I\right] \\ &= \det\left[2cK^{-1}_{1,n}(z,w)_{(1:4)} + Y_2(1)\right],\end{aligned} \tag{7.17}$$

for $w = \pm 1$, since $Y_2(1)Y_2(-1) = I$ and $\det Y_2(1) = 1$. Here, $K^{-1}_{1,n}(z,w)_{(1:4)}$ is the submatrix of $K^{-1}_{1,n}(z,w)$ comprising the rows and columns indexed by the four vertices incident with the e_i, see Figure 5.3.

By an explicit diagonalization of $K^{-1}_{1,n}$ as in [8, Sect. 7], for any two vertices u, v in the same fundamental domain, the limit

$$\lim_{n\to\infty}[K^{-1}_{1,n}(z,w)]_{u,v} = \frac{1}{2\pi}\int_0^{2\pi}[K_1^{-1}(z,e^{i\theta})]_{u,v}\,d\theta \tag{7.18}$$

exists and is independent of the choice of $w = \pm 1$. The proof of the next lemma is deferred until the current proof is completed.

Lemma 7.6. *For $z \in \mathbb{C}$, the limit*

$$\delta(z,w) = \lim_{n\to\infty}\frac{\det K^*_{1,n}(z,w)}{\det K_{1,n}(z,w)} \tag{7.19}$$

satisfies $\delta(z,-1) = \delta(z,1) = \pm 1$.

We deduce that

$$\begin{aligned}\det\psi(z) &= \lim_{n\to\infty}\det\left[Y_2(1) + 2cK^{-1}_{1,n}(z,1)_{(1:4)}\right] && \text{by (7.14), (7.15), (7.18)} \\ &= \delta(z,1) = \pm 1 && \text{by (7.17) and Lemma 7.6.}\end{aligned}$$

Setting $z = 1$, we have by (7.19) that $\det\psi(1) \geq 0$ since it is the limit of a ratio of determinants of two anti-symmetric matrices. By (7.14) and the forthcoming (7.25), ψ is continuous on the unit circle when the spectral curve does not intersect $\mathbb{T}^2$, and the claim follows. (Note that (7.25) is a general fact whose proof does not depend on Lemma 7.5.) Therefore, $\psi(z) = 1$ for $|z| = 1$. □

Proof of Lemma 7.6. By (7.17)–(7.18), $\delta(z,-1) = \delta(z,1) =: \delta(z)$, say. We claim that

$$\det K^*_{1,n}(z,-1) = \det K_{1,n}(z,1), \qquad \det K^*_{1,n}(z,1) = \det K_{1,n}(z,-1). \tag{7.20}$$

By (7.19)–(7.20), $\delta(z,-1) = 1/\delta(z,1)$, so that $\delta(z) = \pm 1$ as claimed.

We prove (7.20) next. Each non-vanishing term in the expansion of $\det K^*_{1,n}(z,-1)$ (respectively, $\det K_{1,n}(z,1)$) corresponds to a cycle configuration on $\mathbb{H}_{1,n,\Delta}$, that is, a configuration of cycles and doubled edges in which each vertex has two incident edges. We may check, by an explicit consideration of the cases that can arise, that every corresponding pair of monomials in the two expansions have the same sign, and the first equation follows.

Here are some further details. Let C be an oriented cycle of $\mathbb{H}^*_{1,n,\Delta}$ viewed as an unoriented graph. It suffices that C contributes the same sign on both sides of (7.20). Let $c(C)$ (respectively, $w(C)$) be the number of c-type (respectively, w-type) edges crossed by C. By a consideration of parity, $c(C)$ is even if and only if $w(C)$ is even, and in this case C contributes the same sign. We claim that $w(C) = 1$ if $c(C) = 1$. It is standard that C is either contractible or essential, and that C, if essential, has homology type ± 1 in the direction γ_x. Therefore, $w(C) = 1$, and the claim follows. The second equation of (7.20) follows similarly. □

We remind the reader of Widom's theorem.

Theorem 7.7 (Widom [37, 38])**.** *Let $T_m(\xi)$ be a finite block Toeplitz matrix with given symbol ξ and $m \times m$ blocks. Assume*

$$\sum_{k=-\infty}^{\infty} \|\xi_k\| + \left(\sum_{k=-\infty}^{\infty} |k| \cdot \|\xi_k\|^2 \right)^{\frac{1}{2}} < \infty,$$

$$\det \xi(e^{i\theta}) \neq 0, \qquad \frac{1}{2\pi} \Delta_{0 \le \theta \le 2\pi} \arg \det \xi(e^{i\theta}) = 0,$$

where $\|\cdot\|$ denotes Hilbert–Schmidt norm, ξ_k is the kth Fourier coefficient of ξ, and

$$\frac{1}{2\pi} \Delta_{0 \le \theta \le 2\pi} \arg \det \xi(e^{i\theta}) = \frac{1}{2\pi i} \int_{|\zeta|=1} d\zeta \, \frac{\partial}{\partial \zeta} \log \det \xi(\zeta).$$

Then

$$\lim_{m \to \infty} \frac{\det T_m(\xi)}{G(\xi)^{m+1}} = E(\xi),$$

where

$$G(\xi) = \exp\left\{ \frac{1}{2\pi} \int_0^{2\pi} \log \det \xi(e^{i\theta}) \, d\theta \right\}, \tag{7.21}$$

$$E(\xi) = \det\left[T(\xi) T(\xi^{-1}) \right], \tag{7.22}$$

and the last det *refers to the determinant defined for operators on Hilbert space differing from the identity by an operator of trace class.*

We note that, when the spectral curve does not intersect the unit torus, ψ given by (7.14) is a smooth matrix-valued function on the unit circle, whence

$$\|\psi_k\| \le C\alpha^k,$$

for some $k > 0$, $\alpha \in (0,1)$, where ψ_k is the kth Fourier coefficient of ψ.

Proof of Theorem 7.1. This holds as in the proofs of [24, Lemmas 4.4–4.7], and the full details are omitted. Here is an outline.

The symbol ψ is a 4×4 matrix-valued function. Let n be the number of NW edges in the path of (3.1) connecting e and f. By the computations of Section 7 (see (7.9) and (7.14)),

$$\langle \sigma_e \sigma_f \rangle^2 = \det T_n(\psi), \tag{7.23}$$

where $T(\psi)$ is an infinite block Toeplitz matrix with symbol ψ, and $T_n(\psi)$ is a truncated block Toeplitz matrix consisting of the first $n \times n$ blocks of $T(\psi)$ (so that $T_n(\psi)$ is a $4n\times 4n$ matrix). By Lemma 7.5, when the spectral curve does not intersect the unit torus $\mathbb{T}^2$, we have $G(\psi) = 1$, where $G(\psi)$ is given in (7.21). By Theorem 7.7,

$$\Lambda(a,b,c) = \lim_{n\to\infty} \det T_n(\psi) = E(\psi), \tag{7.24}$$

where $E(\psi)$ is given in (7.22).

Non-analyticity of Λ may arise only as follows. One may write

$$[K_1^{-1}(z,w)]_{i,j} = \frac{Q_{i,j}(z,w)}{P(z,w)}, \tag{7.25}$$

where $Q_{i,j}(z,w)$ is a Laurent polynomial in z, w derived in terms of certain cofactors of $K_1(z,w)$, and $P(z,w) = \det K_1(z,w)$ is the characteristic polynomial of the dimer model on $\mathbb{H}_{n,\Delta}$. It follows that Λ is analytic when $P(z,w)$ has no zeros on the unit torus $\mathbb{T}^2$. The last occurs only under the condition of Proposition 5.1, and the claim follows. □

8. Proof of Theorem 3.1(d)

We develop the method of proof of Widom's formula, Theorem 7.7, see [37, 38]. For a positive integer r, let $A_r \cap K_r$ be the Banach algebra of $r \times r$ matrix-valued functions on the unit circle under the norm

$$\|\phi\| = \sum_{k=-\infty}^{\infty} \|\phi_k\| + \left(\sum_{k=-\infty}^{\infty} |k| \cdot \|\phi_k\|^2 \right)^{\frac{1}{2}},$$

where ϕ_k is the kth Fourier coefficient of the matrix-valued function ϕ. Note that the trigonometric polynomials are dense in $A_r \cap K_r$.

We recall (7.23) from the last section, and note that ψ is a matrix-valued function in $A_4 \cap K_4$. Let $H(\psi)$ be the Hankel matrix with symbol ψ,

$$H(\psi) = \big(\psi_{i+j+1}\big)_{0\le i,j<\infty},$$

and write

$$\widetilde{\psi}(z) = \psi(z^{-1}). \tag{8.1}$$

Assume first that the operator $T(\widetilde{\psi})$ is invertible. This is equivalent to assuming that the matrix-valued function ψ has a factorization of the form

$$\psi = \psi_+\psi_-,$$

where the $\psi_\pm$ are invertible in $A_4 \cap K_4$, and the $\psi_+^{\pm 1}$ (respectively, $\psi_-^{\pm 1}$) have Fourier coefficients that vanish for negative (respectively, positive) indices. As in [38, Sect. 3], we have

$$\frac{\det T_n(\psi)}{G(\psi)^{n+1}} = \det\Big(I - P_nH(\psi)H(\widetilde{\psi}_-^{-1})P_nT(\psi_+^{-1})P_n\Big),$$

where P_nA is the submatrix of A consisting of its first nr rows, and BP_n is the submatrix of B consisting of its first nr columns. Recall that G is given by (7.21).

For a compact operator A on a Hilbert space, and $1 \le p \le \infty$, let $\|A\|_p$ denote the p-norm of the eigenvalues of $(A^*A)^{\frac{1}{2}}$, where A^* is the conjugate transpose of A. As in [38, Sect. 2],

$$\begin{aligned}\|BAC\|_p &\le \|A\|_p\|B\|_\infty\|C\|_\infty,\\ \|AB\|_1 &\le \|A\|_2\|B\|_2.\end{aligned}$$

Therefore,

$$\begin{aligned}&\Big\|H(\psi)H(\widetilde{\psi}_-^{-1})P_nT(\psi_+^{-1}) - H(\psi)H(\widetilde{\psi}_-^{-1})T(\psi_+^{-1})\Big\|_1\\ &\qquad= \big\|H(\psi)H(\widetilde{\psi}_-^{-1})(P_n - I)T(\psi_+^{-1})\big\|_1\\ &\qquad\le \big\|H(\psi)H(\widetilde{\psi}_-^{-1})(P_n - I)\big\|_1 \cdot \|T(\psi_+^{-1})\|_\infty\\ &\qquad\le \|H(\psi)\|_2 \cdot \|H(\widetilde{\psi}_-^{-1})(P_n - I)\|_2 \cdot \|T(\psi_+^{-1})\|_\infty.\end{aligned}$$

We recall from Proposition 5.1 that, when $a \ge b, c > 0$ and

$$\sqrt{a} \ne \sqrt{b} + \sqrt{c}, \qquad \sqrt{c} \ne \sqrt{a} + \sqrt{b},$$

the characteristic polynomial $P(z, w)$ has no zeros on the unit torus. As in Section 7, $\psi(\xi)$ is a matrix-valued function defined on the unit circle, each entry of which

has the form

$$\frac{1}{2\pi}\int_0^{2\pi}\frac{Q(\xi,e^{i\phi})}{P(\xi,e^{i\phi})}\,d\phi,$$

where $P(z,w)$ is the characteristic polynomial, and $Q(z,w)$ is a Laurent polynomial. When $P(z,w)$ has no zeros on the unit torus, $\psi(\xi)$ is a C^∞ function on the unit circle, and the nth Fourier coefficient of $\psi(\xi)$ decays exponentially to 0 as $|n|\to\infty$. Moreover, by the arguments of [38, p. 10], when $T(\widetilde{\psi})$ is invertible, $\widetilde{\psi}_-^{-1}$ is a matrix-valued function whose sequence of non-negative Fourier coefficients is $T^{-1}(\widetilde{\psi})(I,0,0,\dots)$. By [33, Thm 1.3], the entries in the first column of $T(\widetilde{\psi})^{-1}$ decay exponentially as the entry moves away from the diagonal, whence the nth Fourier coefficient of $\widetilde{\psi}_-^{-1}$ decays to zero exponentially as $|n|\to\infty$.

Let $\mathrm{Tr}(A)$ be the trace of A. There exists $0<\beta_1<1$ such that

$$\begin{aligned}\|T(\psi_+^{-1})\|_\infty &< \infty,\\ \|H(\psi)\|_2 &= \big[\mathrm{Tr}(H^*(\psi)H(\psi))\big]^{\frac{1}{2}} < \infty,\\ \|H(\widetilde{\psi}_-^{-1})(P_n-I)\|_2 &= \mathrm{Tr}\big[(P_n-I)H^*(\widetilde{\psi}_-^{-1})H(\widetilde{\psi}_-^{-1})(P_n-I)\big] < \beta_1^n.\end{aligned}$$

By explicit computations (see [38]),

$$H(\psi)H(\widetilde{\psi}_-^{-1})T(\psi_+^{-1}) = H(\psi)H(\widetilde{\psi}^{-1}),$$

and, moreover,

(8.2)

$$\begin{aligned}&\Big\|P_nH(\psi)H(\widetilde{\psi}^{-1})P_n - H(\psi)H(\widetilde{\psi}^{-1})\Big\|_1\\ &\qquad\le \big\|P_nH(\psi)H(\widetilde{\psi}^{-1})(P_n-I)\big\|_1 + \big\|(P_n-I)H(\psi)H(\widetilde{\psi}^{-1})\big\|_1\\ &\qquad\le \|P_n\|_\infty\cdot\|H(\psi)H(\widetilde{\psi}^{-1})(P_n-I)\|_1 + \|(P_n-I)H(\psi)\|_2\cdot\|H(\widetilde{\psi}^{-1})\|_2\\ &\qquad\le \|H(\psi)\|_2\cdot\|H(\widetilde{\psi}^{-1})(P_n-I)\|_2 + \|(P_n-I)H(\psi)\|_2\cdot\|H(\widetilde{\psi}^{-1})\|_2\\ &\qquad\le \beta_2^n,\end{aligned}$$

where $0<\beta_2<1$.

The following cases may occur:

I. $I-H(\psi)H(\widetilde{\psi}^{-1})$ is invertible,
II. $I-H(\psi)H(\widetilde{\psi}^{-1})$ is not invertible.

Assume Case I occurs. By the formula of [12, p. 116],

$$\begin{aligned}(8.3)\qquad &\Big|\det\big(I - P_nH(\psi)H(\widetilde{\psi}_-^{-1})P_nT(\psi_+^{-1})P_n\big) - \det\big(I - H(\psi)H(\widetilde{\psi}^{-1})\big)\Big| \\ &\qquad\qquad \le e^{\|H(\psi)H(\widetilde{\psi}^{-1})\|_1}(e^{Q_n} - 1) \\ &\qquad\qquad \le \beta_3^n,\end{aligned}$$

where

$$Q_n := \Big\|\big(I - H(\psi)H(\widetilde{\psi}^{-1})\big)^{-1}\Big(P_nH(\psi)H(\widetilde{\psi}_-^{-1})P_nT(\widetilde{\psi}_+^{-1})P_n - H(\psi)H(\widetilde{\psi}^{-1})\Big)\Big\|_1$$

and $0 < \beta_3 < 1$.

Assume Case II occurs. We follow the approach of [12, pp. 116–117]. When $I - H(\psi)H(\widetilde{\psi}^{-1})$ is not invertible, the point 1 is an isolated eigenvalue of finite type for $H(\psi)H(\widetilde{\psi}^{-1})$. Let P be the corresponding Riesz projection, and put $H_1 = \operatorname{Im} P$, $H_2 = \operatorname{Ker} P$, so that H_1 is finite-dimensional. For simplicity, we write

$$\begin{aligned}F_n &:= P_nH(\psi)H(\widetilde{\psi}_-^{-1})P_nT(\psi_+^{-1})P_n, \\ A &:= H(\psi)H(\widetilde{\psi}^{-1}).\end{aligned}$$

With respect to the decomposition $H = H_1 \oplus H_2$, we have

$$F_n = \begin{pmatrix} K_{11}^{(n)} & K_{12}^{(n)} \\ K_{21}^{(n)} & K_{22}^{(n)} \end{pmatrix}, \qquad A = \begin{pmatrix} A_{11} & 0 \\ 0 & A_{22} \end{pmatrix},$$

and it follows from arguments similar to (8.2) that

$$\|F_n - A\|_2 \le \|F_n - A\|_1 \le \beta_4^n,$$

for some $0 < \beta_4 < 1$. Moreover,

$$(F_n - A)^*(F_n - A) = \begin{pmatrix} L_1 & 0 \\ 0 & L_2 \end{pmatrix},$$

where

$$\begin{aligned}L_1 &= (K_{11}^{(n)} - A_{11})^*(K_{11}^{(n)} - A_{11}) + (K_{21}^{(n)})^*K_{21}^{(n)}, \\ L_2 &= (K_{12}^{(n)})^*K_{12}^{(n)} + (K_{22}^{(n)} - A_{22})^*(K_{22}^{(n)} - A_{22}).\end{aligned}$$

Therefore,

$$\begin{aligned}\|F_n - A\|_2^2 &= \operatorname{Tr}\Big((K_{11}^{(n)} - A_{11})^*(K_{11}^{(n)} - A_{11})\Big) + \operatorname{Tr}\Big((K_{21}^{(n)})^*K_{21}^{(n)}\Big) \\ &\qquad + \operatorname{Tr}\Big((K_{22}^{(n)} - A_{22})^*(K_{22}^{(n)} - A_{22})\Big) + \operatorname{Tr}\Big((K_{12}^{(n)})^*K_{12}^{(n)}\Big) \\ &= \|K_{11}^{(n)} - A_{11}\|_2^2 + \|K_{21}^{(n)}\|_2^2 + \|K_{12}^{(n)}\|_2^2 + \|K_{22}^{(n)} - A_{22}\|_2^2.\end{aligned}$$

Hence,

$$\begin{aligned}\|K_{11}^{(n)} - A_{11}\|_2 &\le \beta_4^n,\\ \|K_{12}^{(n)}\|_2 &\le \beta_4^n,\\ \|K_{21}^{(n)}\|_2 &\le \beta_4^n.\end{aligned}$$

As in [12, pp. 116–117],

$$\det(I - F_n) = \det\left(I_1 - K_{11}^{(n)} + K_{12}^{(n)}(I_2 - K_{22}^{(n)})^{-1}K_{21}^{(n)}\right)\det\left(I_2 - K_{22}^{(n)}\right),$$

and

$$\lim_{n\to\infty}\det\left(I_2 - K_{22}^{(n)}\right) = \det(I - A_{22}).$$

Moreover,

$$\begin{aligned}&\left\|I_1 - K_{11}^{(n)} + K_{12}^{(n)}(I_2 - K_{22}^{(n)})^{-1}K_{21}^{(n)} - (I_1 - A_{11})\right\|_1\\ &\qquad\le \|K_{11}^{(n)} - A_{11}\|_1 + \|K_{12}^{(n)}\|_2 \cdot \|I_2 - K_{22}^{(n)}\|_\infty \cdot \|K_{21}^{(n)}\|_2\\ &\qquad\le \beta_6^n,\end{aligned}$$

for some $0 < \beta_6 < 1$. Since $I_1 - K_{11}^{(n)} + K_{12}^{(n)}(I_2 - K_{22}^{(n)})^{-1}K_{21}^{(n)}$ is a finite matrix, all the norms are equivalent, we have

$$\left|\det\left(I_1 - K_{11}^{(n)} + K_{12}^{(n)}(I_2 - K_{22}^{(n)})^{-1}K_{21}^{(n)}\right) - \det(I_1 - A_{11})\right| \le \beta_7^n,$$

for some $0 < \beta_7 < 1$.

Since (by Lemma 7.5) $G(\psi) = 1$, we obtain that, when $T(\widetilde{\psi})$ is invertible, $\langle\sigma_e\sigma_f\rangle^2$ converges to its limit exponentially fast in the limit as $|e - f| \to \infty$. This completes the consideration of Case II.

Assume now that $T(\widetilde{\psi})$ is not invertible. Since $T(\widetilde{\psi})$ is Fredholm of index 0, by [38], there exists ϕ with only finitely many non-zero Fourier coefficients, such that $T(\widetilde{\psi} + \epsilon\widetilde{\phi})$ is invertible for sufficiently small $\epsilon \neq 0$. Therefore,

$$\lim_{n\to\infty}\frac{\det T_n[\psi + \epsilon\phi]}{G(\psi + \epsilon\phi)^{n+1}} = \det\left[T(\psi + \epsilon\phi)T\left([\psi + \epsilon\phi]^{-1}\right)\right],$$

for ϵ belonging to some punctured disk with centre 0. Using the same arguments as above we obtain that, for sufficiently small $|\epsilon| > 0$,

$$\left|\frac{\det T_n(\psi + \epsilon\phi)}{G(\psi + \epsilon\phi)^{n+1}} - \lim_{n\to\infty}\frac{\det T_n(\psi + \epsilon\phi)}{G(\psi + \epsilon\phi)^{n+1}}\right| \le \beta_5^n \tag{8.4}$$

for some $0 < \beta_5 < 1$ independent of ϵ. Since the component functions on the left side of (8.4) are analytic on the above disk, by the maximal principle, (8.4) holds

for $\epsilon = 0$ also. Hence $\langle \sigma_e \sigma_f \rangle^2$ converges to its limit exponentially fast. The proof is complete.

9. Proof of Theorem 3.2

It is slightly more convenient to work with horizontal edges rather than NW edges, and there is no essential difference in the proof. Let $e, f \in \mathbb{E}$ be horizontal edges. There exists a horizontal edge $g \in \mathbb{E}$ such that: e and g (respectively, f and g) are connected by a path l_{eg} (respectively, l_{fg}) of $A\mathbb{H}$ comprising only horizontal and NW (respectively, NE) edges, and the unique common edge of l_{eg} and l_{fg} is g. Let $m+1$ (respectively, $n+1$) be the number of horizontal edges in l_{eg} (respectively, l_{fg}). Write $m \wedge n = \min\{m, n\}$ and $m \vee n = \max\{m, n\}$.

Theorem 9.1. *Assume the parameters of the 1-2 model satisfy*

$$a \geq b > 0, \quad c > 0, \quad \sqrt{a} \neq \sqrt{b} + \sqrt{c}, \quad \sqrt{c} \neq \sqrt{a} + \sqrt{b}. \tag{9.1}$$

(a) *The limit*

$$\Lambda(a, b, c) := \lim_{m,n \to \infty} \langle \sigma_e \sigma_f \rangle^2$$

exists, and

$$\left| \langle \sigma_e \sigma_f \rangle^2 - \Lambda \right| \leq C \alpha^{m \wedge n}, \tag{9.2}$$

where $C > 0$, $\alpha \in (0, 1)$ are constants independent of m, n.

(b) *If, in addition, $\sqrt{a} < \sqrt{b} + \sqrt{c}$ and $\sqrt{c} < \sqrt{a} + \sqrt{b}$, then $C > 0$, $\alpha \in (0, 1)$ may be chosen such that*

$$|\langle \sigma_e \sigma_f \rangle| \leq C \alpha^{|e-f|}. \tag{9.3}$$

Proof. (a) By a computation similar to that leading to (7.9), $\langle \sigma_e \sigma_f \rangle^2$ may be expressed in the form

$$\langle \sigma_e \sigma_f \rangle^2 = \det \begin{pmatrix} T_m(\psi_1) & A_{m,n} \\ B_{n,m} & T_n(\psi_2) \end{pmatrix},$$

where ψ_i is a 4×4 matrix-valued function (see (7.14)), $T_r(\psi_i)$ is a $4r \times 4r$ truncated block Toeplitz matrix with symbol ψ_i, and $A_{m,n}$ (respectively, $B_{n,m}$) is a $4m \times 4n$ (respectively, $4n \times 4m$) matrix with entries satisfying

$$|A_{m,n}(i, j)| \leq C \beta_1^{i+j}, \qquad |B_{n,m}(i, j)| \leq C \beta_1^{i+j},$$

where $C > 0$, $\beta_1 \in (0, 1)$ are constants independent of i, j.

Let ϕ_1, ϕ_2 be two matrix-valued functions defined on the unit circle with only finitely many non-vanishing Fourier coefficients, such that $T(\widetilde{\psi}_1 + \epsilon \widetilde{\phi}_1)$ and $T(\widetilde{\psi}_2 + \epsilon \widetilde{\phi}_2)$

are invertible for complex $\epsilon \neq 0$ with sufficiently small modulus (recall (8.1)). Let $\epsilon > 0$ be given accordingly, and let

$$\psi_{i,\epsilon} = \varphi_i + \epsilon\phi_i, \qquad i = 1, 2.$$

Since $T(\widetilde{\psi}_{i,\epsilon})$ is invertible, we have (as in Section 8) that

$$\psi_{i,\epsilon} = \psi_{i,\epsilon,+}\psi_{i,\epsilon,-}, \qquad i = 1, 2,$$

where the $\psi_{i,\epsilon,\pm}$ are invertible in $A_4 \cap K_4$, and $\psi_{i,\epsilon,+}^{\pm 1}$ (respectively, $\psi_{i,\epsilon,-}^{\pm 1}$) have Fourier coefficients that vanish for negative (respectively, positive) indices.

Subject to (9.1), by Proposition 5.1 the spectral curve has no zeros on the unit torus. As explained after Theorem 7.7, the entries of the Toeplitz matrix (Fourier coefficients of a smooth function on the unit circle) decay exponentially as their distances from the diagonal go to infinity.

By computations similar to those of [38, p. 8],

$$\begin{aligned}(9.4)\qquad &\begin{pmatrix} T_m(\psi_{1,\epsilon}) & A_{m,n} \\ B_{n,m} & T_n(\psi_{2,\epsilon}) \end{pmatrix} \begin{pmatrix} T_m(\psi_{1,\epsilon,-}^{-1})T_m(\psi_{1,\epsilon,+}^{-1}) & 0 \\ 0 & T_n(\psi_{2,\epsilon,-}^{-1})T_n(\psi_{2,\epsilon,+}^{-1}) \end{pmatrix} \\ &\quad = \begin{pmatrix} T_m(\psi_{1,\epsilon})T_m(\psi_{1,\epsilon,-}^{-1})T_m(\psi_{1,\epsilon,+}^{-1}) & A_{m,n}T_n(\psi_{2,\epsilon,-}^{-1})T_n(\psi_{2,\epsilon,+}^{-1}) \\ B_{n,m}T_m(\psi_{1,\epsilon,-}^{-1})T_m(\psi_{1,\epsilon,+}^{-1}) & T_n(\psi_{2,\epsilon})T_n(\psi_{2,\epsilon,-}^{-1})T_n(\psi_{2,\epsilon,+}^{-1}) \end{pmatrix} \\ &\quad = I_{4m+4n} - S_{m,n},\end{aligned}$$

where I_r is the $r \times r$ identity matrix and

$$S_{m,n} = \begin{pmatrix} P_m H(\psi_{1,\epsilon}) H(\widetilde{\psi}_{1,\epsilon,-}^{-1}) P_m T_m(\psi_{1,\epsilon,+}^{-1}) & -A_{m,n}T_n(\psi_{2,\epsilon,-}^{-1})T_n(\psi_{2,\epsilon,+}^{-1}) \\ -B_{n,m}T_m(\psi_{1,\epsilon,-}^{-1})T_m(\psi_{1,\epsilon,+}^{-1}) & P_n H(\psi_{2,\epsilon}) H(\widetilde{\psi}_{2,\epsilon,-}^{-1}) P_n T_n(\psi_{2,\epsilon,-}^{-1}) \end{pmatrix}.$$

We now take determinants of (9.4). As in [38, p. 8],

$$\begin{aligned}\det[T_m(\psi_{1,\epsilon,-}^{-1})] \det[T_m(\psi_{1,\epsilon,+}^{-1})] &= G(\psi_{1,\epsilon,-}^{-1})^{m+1} G(\psi_{1,\epsilon,+}^{-1})^{m+1} \\ &= \frac{1}{G(\psi_{1,\epsilon})^{m+1}},\end{aligned}$$

whence

$$(9.5)\qquad \frac{1}{G(\psi_{1,\epsilon})^{m+1} G(\psi_{2,\epsilon})^{n+1}} \det \begin{pmatrix} T_m(\psi_{1,\epsilon}) & A_{m,n} \\ B_{n,m} & T_n(\psi_{2,\epsilon}) \end{pmatrix} = \det\left(I_{4m+4n} - S_{m,n}\right).$$

Let

$$(9.6)\qquad S = \begin{pmatrix} H(\psi_{1,\epsilon}) H(\widetilde{\psi}_{1,\epsilon,-}^{-1}) T(\psi_{1,\epsilon,+}^{-1}) & -AT(\psi_{2,\epsilon,-}^{-1}) T(\psi_{2,\epsilon,+}^{-1}) \\ -BT(\psi_{1,\epsilon,-}^{-1}) T(\psi_{1,\epsilon,+}^{-1}) & H(\psi_{2,\epsilon}) H(\widetilde{\psi}_{2,\epsilon,-}^{-1}) T(\psi_{2,\epsilon,-}^{-1}) \end{pmatrix},$$

where A and B are infinite matrices obtained as the limits of $A_{m,n}$ and $B_{n,m}$, as $m, n \to \infty$. Note that S is a trace-class operator. Therefore, $\det(I - S)$ is well-defined and complex analytic in a, b, c, whenever the entries of S are analytic in a, b, c (see [13], and also [12, Lemma 3.1] and [24, Lemma 4.6]). Then,

$$\begin{aligned}\|S_{m,n} - S\|_1 \le{}& \left\|A_{m,n}T_n(\psi_{2,\epsilon,-}^{-1})T_n(\psi_{2,\epsilon,+}^{-1}) - AT(\psi_{2,\epsilon,-}^{-1})T(\psi_{2,\epsilon,+}^{-1})\right\|_1\\ &+ \left\|B_{n,m}T_m(\psi_{1,\epsilon,-}^{-1})T_m(\psi_{1,\epsilon,+}^{-1}) - BT(\psi_{1,\epsilon,-}^{-1})T(\psi_{1,\epsilon,+}^{-1})\right\|_1\\ &+ \left\|P_mH(\psi_{1,\epsilon})H(\widetilde{\psi}_{1,\epsilon,-}^{-1})P_mT_m(\psi_{1,\epsilon,+}^{-1}) - H(\psi_{1,\epsilon})H(\widetilde{\psi}_{1,\epsilon,-}^{-1})T(\psi_{1,\epsilon,+}^{-1})\right\|_1\\ &+ \left\|P_nH(\psi_{2,\epsilon})H(\widetilde{\psi}_{2,\epsilon,-}^{-1})P_nT_n(\psi_{2,\epsilon,-}^{-1}) - H(\psi_{2,\epsilon})H(\widetilde{\psi}_{2,\epsilon,-}^{-1})T(\psi_{2,\epsilon,-}^{-1})\right\|_1.\end{aligned}$$

Using similar arguments as in (8.2), we can show that

$$\begin{aligned}\left\|P_mH(\psi_{1,\epsilon})H(\widetilde{\psi}_{1,\epsilon,-}^{-1})P_mT_m(\psi_{1,\epsilon,+}^{-1}) - H(\psi_{1,\epsilon})H(\widetilde{\psi}_{1,\epsilon,-}^{-1})T(\psi_{1,\epsilon,+}^{-1})\right\|_1 &\le \beta_2^m,\\ \left\|P_nH(\psi_{2,\epsilon})H(\widetilde{\psi}_{2,\epsilon,-}^{-1})P_nT_n(\psi_{2,\epsilon,-}^{-1}) - H(\psi_{2,\epsilon})H(\widetilde{\psi}_{2,\epsilon,-}^{-1})T(\psi_{2,\epsilon,-}^{-1})\right\|_1 &\le \beta_2^n,\end{aligned}$$

where $\beta_2 \in (0,1)$ is a constant independent of m, n, ϵ. Moreover,

$$|A(i,j)| \le C\beta_1^{i+j}, \quad |B(i,j)| \le C\beta_1^{i+j}, \quad |T(\psi_*)(i,j)| \le C\beta_3^{|i-j|},$$

subject to (9.1). Here, $\psi_* \in \{\psi_{2,\epsilon,-}^{-1}, \psi_{2,\epsilon,+}^{-1}, \psi_{1,\epsilon,+}^{-1}, \psi_{1,\epsilon,-}^{-1}\}$, and $\beta_1, \beta_3 \in (0,1)$ are independent of i, j, ϵ. Therefore,

$$\begin{aligned}\left|AT(\psi_{2,\epsilon,+}^{-1})T(\psi_{2,\epsilon,-}^{-1})(i,j)\right| &\le C_1\beta_4^{i+j}, & \left|BT(\psi_{1,\epsilon,+}^{-1})T(\psi_{1,\epsilon,-}^{-1})(i,j)\right| &\le C_1\beta_4^{i+j},\\ |AT(\psi_{2,\epsilon,+}^{-1})(i,j)| &\le C_1\beta_4^{i+j}, & |AT(\psi_{2,\epsilon,-}^{-1})(i,j)| &\le C_1\beta_4^{i+j},\\ |BT(\psi_{1,\epsilon,+}^{-1})(i,j)| &\le C_1\beta_4^{i+j}, & |BT(\psi_{1,\epsilon,-}^{-1})(i,j)| &\le C_1\beta_4^{i+j},\end{aligned}$$

where $C_1 > 0$, $\beta_4 \in (0,1)$ are constants independent of i, j, ϵ.

Hence,

$$\left\|P_mAT(\psi_{2,\epsilon,+}^{-1})T(\psi_{2,\epsilon,-}^{-1})P_n - AT(\psi_{2,\epsilon,-}^{-1})T(\psi_{2,\epsilon,+}^{-1})\right\|_1 \le C_2\beta_5^{m\wedge n},$$

where $C_2 > 0$, $\beta_5 \in (0,1)$ are constants independent of i, j, ϵ.

Moreover,

$$\begin{aligned}&\left\|P_mAT(\psi_{2,\epsilon,-}^{-1})P_nT(\psi_{2,\epsilon,-}^{-1})P_n - P_mAT(\psi_{2,\epsilon,-}^{-1})T(\psi_{2,\epsilon,+}^{-1})P_n\right\|_1\\ &\quad= \|P_mAT(\psi_{2,\epsilon,-}^{-1})(P_n - I)T(\psi_{2,\epsilon,+}^{-1})P_n\|_1\\ &\quad\le \|P_mAT(\psi_{2,\epsilon,-}^{-1})(P_n - I)\|_1 \cdot \|T(\psi_{2,\epsilon,+}^{-1})P_n\|_\infty\\ &\quad\le C_3\beta_6^n,\end{aligned}$$

and

$$\begin{aligned}\Big\| P_m A P_n T(\psi_{2,\epsilon,-}^{-1}) P_n T(\psi_{2,\epsilon,-}^{-1}) P_n - P_m A T(\psi_{2,\epsilon,-}^{-1}) P_n T(\psi_{2,\epsilon,+}^{-1}) P_n \Big\|_1 \\ = \| P_m A (P_n - I) T(\psi_{2,\epsilon,-}^{-1}) P_n T(\psi_{2,\epsilon,+}^{-1}) P_n \|_1 \\ \le \| P_m A (P_n - I) \|_1 \cdot \| T(\psi_{2,\epsilon,-}^{-1}) P_n T(\psi_{2,\epsilon,+}^{-1}) P_n \|_\infty \\ \le C_3 \beta_6^n,\end{aligned}$$

where $C_3 > 0$, $\beta_6 \in (0,1)$ are constants independent of m, n, ϵ.

We consider the following cases:

I. $I - S$ is invertible,
II. $I - S$ is not invertible.

If Case I occurs, following arguments similar to those of Section 8,

$$\big|\det(I - S_{m,n}) - \det(I - S)\big| \le C_4 \beta_7^{m \wedge n}, \tag{9.7}$$

where $C_4 > 0$, $\beta_7 \in (0,1)$ are constants independent of m, n, ϵ. *If Case II occurs*, by considering the Riesz projection and following similar arguments,

$$\big|\det(I - S_{m,n}) - \det(I - S)\big| \le C_5 \beta_8^{m \wedge n}, \tag{9.8}$$

where $C_5 > 0$, $\beta_8 \in (0,1)$ are constants independent of m, n, ϵ.

Letting $\epsilon \to 0$ and using analyticity (as in Section 8) subject to (9.1), we have

$$\Lambda := \lim_{m,n \to \infty} \langle \sigma_e \sigma_f \rangle^2 = \det(I - S)\big|_{\epsilon = 0},$$

by (9.5), (9.7), (9.8) and the fact that $G(\psi_i) = 1$ (the last follows by Lemma 7.5 and (7.21)). Moreover, (10.2) holds.

(b) The above argument applies also when m is fixed and $n \to \infty$. In this case, we replace S in (9.6) by

$$S_m = \begin{pmatrix} P_m H(\psi_{1,\epsilon}) H(\widetilde{\psi}_{1,\epsilon,-}^{-1}) P_m T_m(\psi_{1,\epsilon,+}^{-1}) & -A_{m,\infty} T(\psi_{2,\epsilon,-}^{-1}) T(\psi_{2,\epsilon,+}^{-1}) \\ -B_{\infty,m} T_m(\psi_{1,\epsilon,-}^{-1}) T_m(\psi_{1,\epsilon,+}^{-1}) & H(\psi_{2,\epsilon}) H(\widetilde{\psi}_{2,\epsilon,-}^{-1}) T(\psi_{2,\epsilon,-}^{-1}) \end{pmatrix},$$

where $A_{m,\infty}$, $B_{\infty,m}$ are matrices obtained from $A_{m,n}$, $B_{n,m}$ by letting $n \to \infty$. Now, $\det(I - S_m)$ exists since S_m is a trace-class operator, and

$$\lim_{n \to \infty} \langle \sigma_e \sigma_f \rangle^2 = \det(I - S_m)\big|_{\epsilon = 0}, \qquad m \ge 0, \tag{9.9}$$

as above. We claim that there exists $C > 0$, $\alpha \in (0,1)$, independent of m, n, such that

$$\Big| \langle \sigma_e \sigma_f \rangle^2 - \lim_{n \to \infty} \langle \sigma_e \sigma_f \rangle^2 \Big| \le C \alpha^n, \qquad m, n \ge 0. \tag{9.10}$$

To show (9.10), first, following the same computations as above, we obtain

$$\| S_{m,n} - S_m \|_1 \le C_7 \beta_9^n,$$

for constants $C_7 > 0$, $\beta_9 \in (0,1)$ independent of m, n, ϵ.

We consider the following cases:

I. $I - S$ is invertible,
II. $I - S$ is not invertible.

In Case I, for sufficiently large m, $I - S_m$ is also invertible. Following the arguments of [12, pp. 115–116], we obtain

$$\left|\det(I - S_{m,n}) - \det(I - S_m)\right| \le C_8 \beta_{10}^n,$$

for $C_8 > 0$, $\beta_{10} \in (0,1)$ independent of m, n, ϵ.

In Case II, the point 1 is an isolated eigenvalue of finite type for S. Let P be the corresponding Riesz projection, and put $H_1 = \operatorname{Im} P$, $H_2 = \operatorname{Ker} P$, so that H_1 is finite dimensional. With respect to the decomposition, we have

$$S_{m,n} = \begin{pmatrix} K_{11}^{(m,n)} & K_{12}^{(m,n)} \\ K_{21}^{(m,n)} & K_{22}^{(m,n)} \end{pmatrix}, \qquad S_m = \begin{pmatrix} K_{11}^{(m)} & K_{12}^{(m)} \\ K_{21}^{(m)} & K_{22}^{(m)} \end{pmatrix}.$$

We now follow the argument of [12, pp. 115–116] and the proof in Section 8, to obtain (9.10).

Fix m, and note that $S_m\big|_{\epsilon=0}$ is an operator of trace class. By [24, Thm 4.6] (see also [13]) and (9.9), $\lim_{n\to\infty}\langle\sigma_e\sigma_f\rangle^2 = \det(I - S_m)\big|_{\epsilon=0}$ is analytic in a, b, c subject to

$$a, b, c > 0, \quad \sqrt{a} < \sqrt{b} + \sqrt{c}, \quad \sqrt{b} < \sqrt{a} + \sqrt{c}, \quad \sqrt{c} < \sqrt{a} + \sqrt{b}. \tag{9.11}$$

By Remark 4.2, $\lim_{n\to\infty}\langle\sigma_e\sigma_f\rangle^2 = 0$ when

$$a, b, c > 0, \quad a^2 < b^2 + c^2, \quad b^2 < a^2 + c^2, \quad c^2 < a^2 + b^2. \tag{9.12}$$

The set of (a, b, c) satisfying (9.12) is a subset of the (connected) subset of $\mathbb{R}^3$ given by (9.11), and it follows by analyticity that

$$\lim_{n\to\infty}\langle\sigma_e\sigma_f\rangle^2 = 0, \qquad m \ge 0, \tag{9.13}$$

subject to (9.11).

By the arguments that led to (9.10), there exists $C > 0$, $\alpha \in (0,1)$, independent of m, n, such that, subject to (9.11),

$$\left|\langle\sigma_e\sigma_f\rangle^2 - \lim_{m\to\infty}\langle\sigma_e\sigma_f\rangle^2\right| \le C\alpha^m, \qquad m, n \ge 0, \tag{9.14}$$

and, in addition,

$$\lim_{m\to\infty}\langle\sigma_e\sigma_f\rangle^2 = 0, \qquad n \ge 0, \tag{9.15}$$

We combine (9.10)–(9.15) to obtain

$$\langle\sigma_e\sigma_f\rangle^2 \le C\alpha^{m\vee n},$$

which implies (10.3) with amended C, α.

□

10. Periodic 1-2 models

10.1. **Two-edge correlation for periodic models.** Some of the previous results may be extended to certain periodic models, as explained next. Since each edge of $\mathbb{H}$ touches exactly one white vertex, a 1-2 model may be specified by assigning a parameter-vector (a_w, b_w, c_w) to each *white* vertex w. For $k, l \in \mathbb{N}$, we call the ensuing model $k \times l$ *periodic* if

$$(a_w, b_w, c_w) = (a_v, b_v, c_v), \qquad v = \tau_1^k \tau_2^l w,$$

where the maps τ_i are illustrated in Figure 2.3.

By the techniques of Sections 7, if the parameter-vectors of a periodic model are such that the associated spectral curve does not intersect the unit torus, then the entries of the corresponding inverse Kasteleyn matrix $K^{-1}(v, w)$ converge to 0 exponentially as $|v - w| \to \infty$. Following the procedure of Section 9, we obtain the following (in which the notation of Theorem 9.1 has been adopted).

Theorem 10.1. *Let $k, l \geq 1$. Assume the 1-2 model is $k \times l$ periodic, and the spectral curve does not intersect the unit torus.*

(a) *The limit $\Lambda := \lim_{m,n\to\infty} \langle \sigma_e \sigma_f \rangle^2$ exists, and*

$$\left| \langle \sigma_e \sigma_f \rangle^2 - \Lambda \right| \leq C \alpha^{m \wedge n}, \tag{10.1}$$

where $C > 0$, $\alpha \in (0, 1)$ are constants independent of m, n. If $m = 0$, we have

$$\left| \langle \sigma_e \sigma_f \rangle^2 - \Lambda \right| \leq C \alpha^{n}. \tag{10.2}$$

(b) *If, in addition, $\lim_{|e-f|\to\infty} \langle \sigma_e \sigma_f \rangle^2 = 0$, then $C > 0$, $\alpha \in (0, 1)$ may be chosen such that*

$$|\langle \sigma_e \sigma_f \rangle| \leq C \alpha^{|e-f|}. \tag{10.3}$$

10.2. **1-2 and Ising models with period $k \times 1$.** We discuss a special case of periodic 1-2 models, namely, models with period $k \times 1$. By the forthcoming Theorem 10.2, the spectral curves of such models can intersect the unit torus only at real points. The conclusions of Theorem 10.1 follow whenever the corresponding characteristic polynomial $P(z, w)$ satisfies $P(\pm 1, \pm 1) \neq 0$. Similar arguments are valid for periodic Ising models, as exemplified in the forthcoming Example 10.4, which illuminates the differences between the assumptions of the current paper and those of [29].

Let $k \geq 2$ and consider a $k \times 1$ periodic 1-2 model. Let $\mathbb{H}_\Delta$ be as in Section 5, and let $\mathbb{H}_{\Delta,k,1}$ be the quotient graph of $\mathbb{H}_\Delta$ under the weight preserving action of $\mathbb{Z}^2$.

Note that $\mathbb{H}_{\Delta,k,1}$ is a finite graph that can be embedded in a torus. We can divide $\mathbb{H}_{\Delta,k,1}$ into k parts, each of which is bounded by a quadrilateral region enclosing a NE/SW edge of the original lattice $\mathbb{H}$, see Figure 10.1.

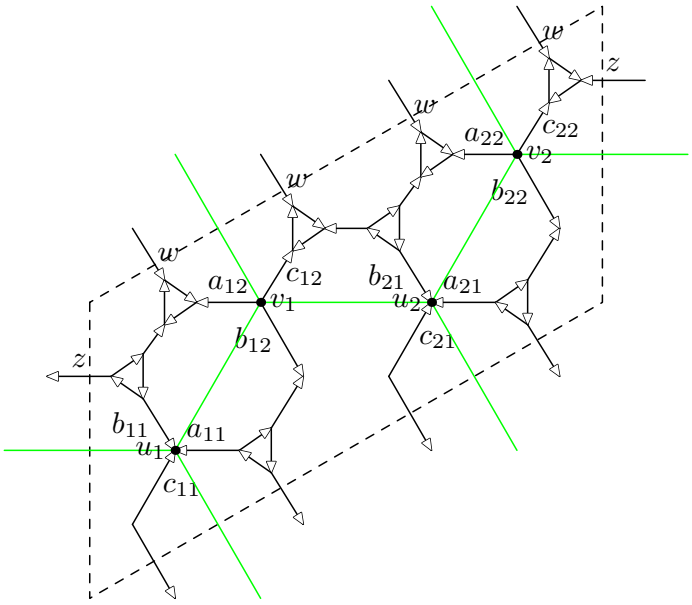

FIGURE 10.1. The decorated graph $\mathbb{H}_{\Delta,2,1}$; the hexagonal lattice $\mathbb{H}$ is represented by green lines.

There are two vertices of $\mathbb{H}$ lying in the ith such quadrilateral region (see Figure 5.1), and to these we assign local weights (a_{i1}, b_{i1}, c_{i1}) and (a_{i2}, b_{i2}, c_{i2}), respectively. As in Section 5.2, we derive the modified weighted adjacency matrix $K(z, w)$ of $\mathbb{H}_{\Delta,k,1}$, with characteristic polynomial $P(z, w)$.

Theorem 10.2. *If the spectral curve* $\{(z, w) : P(z, w) = 0\}$ *intersects the unit torus* $\mathbb{T}^2 = \{(z, w) : |z| = 1, |w| = 1\}$*, the only possible intersection is a single real point.*

Proof. Each term of the determinant $P(z, w)$ falls into one of the following two categories:

1. it occupies each z-edge exactly once,
2. each z-edge is either unoccupied or occupied exactly twice.

Each $k \times 1$ fundamental domain is comprised of k 1×1 blocks. For $1 \le i \le n$, let u_i, v_i be the two vertices of the hexagonal lattice lying in the ith block, see Figure 10.1.

Each configuration in Case 1 consists of a single essential cycle of even length, together with some doubled edges. The partition function of configurations in Case

1 is

$$P_1 = \frac{1}{z}\prod_{i=1}^{k}\left[A_i w + B_i\right] + z\prod_{i=1}^{k}\left[\frac{A_i}{w} + B_i\right],$$

where

$$\begin{aligned} A_i =& -a_{i1}^2 a_{i2} b_{i2} - a_{i1} a_{i2}^2 b_{i1} - a_{i1} b_{i1} b_{i2}^2 + a_{i1} b_{i1} c_{i2}^2 - a_{i2} b_{i1}^2 b_{i2} + a_{i2} b_{i2} c_{i1}^2, \\ B_i =& -a_{i1}^2 a_{i2} c_{i2} - a_{i1} a_{i2}^2 c_{i1} + a_{i1} b_{i2}^2 c_{i1} - a_{i1} c_{i1} c_{i2}^2 + a_{i2} b_{i1}^2 c_{i2} - a_{i2} c_{i1}^2 c_{i2}. \end{aligned}$$

Configurations in Case 2 depend on configurations of each 1×1 block, which are determined by configurations of boundary edges. Let Q_i^{00} (respectively, Q_i^{22}) denote the partition function at the ith block when both its z-edges are unoccupied (respectively, occupied). Let Q_i^{20} (respectively, Q_i^{02}) denote the partition function at the ith block when its left (respectively, right) z-edge is occupied twice, while the right (respectively, left) edge is unoccupied. Then we have

$$\begin{aligned} Q_i^{00} =& \left(a_{i1}a_{i2} - \frac{b_{i1}c_{i2}}{w} + b_{i1}b_{i2} + c_{i1}c_{i2} - b_{i2}c_{i1}w\right) \\ &\times \left(a_{i1}a_{i2} - \frac{b_{i2}c_{i1}}{w} + b_{i1}b_{i2} + c_{i1}c_{i2} - b_{i1}c_{i2}w\right), \\ Q_i^{02} =& W\left[a_{i2}^2 b_{i1}c_{i1} + a_{i1}c_{i2}a_{i2}b_{i1} + a_{i1}b_{i2}a_{i2}c_{i1} + b_{i2}c_{i2}\left(b_{i1}^2 - b_{i1}c_{i1}\left(w + \frac{1}{w}\right) + c_{i1}^2\right)\right], \\ Q_i^{20} =& W\left[a_{i1}^2 b_{i2}c_{i2} + a_{i2}c_{i1}a_{i1}b_{i2} + a_{i2}b_{i1}a_{i1}c_{i2} + b_{i1}c_{i1}\left(b_{i2}^2 - b_{i2}c_{i2}\left(w + \frac{1}{w}\right) + c_{i2}^2\right)\right], \\ Q_i^{22} =& -b_{i1}b_{i2}c_{i1}c_{i2}\left(w - \frac{1}{w}\right)^2 + (a_{i1}b_{i2} + a_{i2}b_{i1})^2 + (a_{i1}c_{i2} + a_{i2}c_{i1})^2 \\ &+ \left(a_{i2}^2 b_{i1}c_{i1} + a_{i1}^2 b_{i2}c_{i2} + a_{i1}a_{i2}b_{i1}c_{i2} + a_{i1}a_{i2}b_{i2}c_{i1}\right)\left(w + \frac{1}{w}\right), \end{aligned}$$

where $W = (w - w^{-1})$.

Let $t_i \in \{0, 2\}$ denote the occupation time of the z-edge connecting the ith 1×1 block and the $[(i+1) \bmod k]$th 1×1 block. The partition function in Case 2 is

$$P_2 = \sum_{t_1,\ldots,t_k \in \{0,2\}} \prod_{i=1}^{i} Q_i^{t_{i-1}t_i}.$$

Let $w = e^{i\phi}$, so that $Q_i^{00}, Q_i^{22} \geq 0$. By periodicity, in each configuration, the number of Q^{02} blocks equals the number of Q^{20} blocks. Therefore in all terms in P_2 where $\sin\phi$ appears, which are exactly the terms where Q^{02} and Q^{20} appear, $\sin\phi$ has even

degree. Moreover, given that all the local weights are strictly positive, each term in the expansion of P_2 with $\sin\phi$ is non-negative. Therefore,

$$P(z,w) = P_1 + P_2 = P_1 + \prod_{i=1}^{k} Q_i^{00} + \prod_{i=1}^{k} Q_i^{22} + F(w),$$

where $F(w) \geq 0$ is the sum of all terms in P_2 in which Q^{02} and Q^{20} appear at some 1×1 blocks. Let $G(z,w) = z[P(z,w) - F(w)]$. For given w, $G(z,w)$ is a quadratic polynomial in z. Let

$$C_0 = \prod_{i=1}^{k} [A_i w + B_i], \qquad C_1 = \prod_{i=1}^{k} Q_i^{00} + \prod_{i=1}^{k} Q_i^{22}.$$

The roots of $G(\cdot, w)$ are

$$z^{\pm} = \frac{C_1 \pm \sqrt{C_1^2 - 4|C_0|^2}}{2\overline{C_0}}. \tag{10.4}$$

Let $w = e^{i\phi}$, and note that

$$C_1^2 - 4|C_0|^2 \geq 4\left(\prod_{i=1}^{k}[Q_i^{00}Q_i^{22}] - \prod_{i=1}^{k}\left[A_i^2 + B_i^2 + 2A_iB_i\cos\phi\right]\right).$$

Moreover,

$$\begin{aligned} &Q_i^{00}Q_i^{22} - \left(A_i^2 + B_i^2 + 2A_iB_i\cos\phi\right) \\ &\quad = -\left(w - \frac{1}{w}\right)^2 \\ &\qquad \times \left(a_{i1}^2 b_{i2}c_{i2} + a_{i2}c_{i1}a_{i1}b_{i2} + a_{i2}b_{i1}a_{i1}c_{i2} + b_{i1}c_{i1}\left(b_{i2}^2 + c_{i2}^2 - 2b_{i2}c_{i2}\cos\theta\right)\right) \\ &\qquad \times \left(a_{i2}^2 b_{i1}c_{i1} + a_{i1}c_{i2}a_{i2}b_{i1} + a_{i1}b_{i2}a_{i2}c_{i1} + b_{i2}c_{i2}(b_{i1}^2 - 2b_{i1}c_{i1}\cos\theta - c_{i1}^2)\right). \end{aligned}$$

Let $a_i, b_i, c_i > 0$. Then $C_1^2 - 4|C_0|^2 \geq 0$ with equality only if w is real. If $C_1^2 - 4|C_0|^2 > 0$, then $|z^{\pm}| \neq 1$ and $G(\cdot, w)$ has no zeros on the unit circle. Hence $G(z,w)$ has no zeros on $\mathbb{T} \times (\mathbb{T} \setminus \{\pm 1\})$. There exists at least one pair $\theta, \tau \in \{0,1\}$ such that

$$G((-1)^\theta, (-1)^\tau) = \det K((-1)^\theta, (-1)^\tau) > 0,$$

hence $G(z,w) \geq 0$ on $\mathbb{T}^2$, with equality only if w is real. By (10.4), when w is real and $C_1^2 - 4|C_0|^2 = 0$, then $z^+ = z^-$ is real. Therefore, the only possible intersection of $P(z,w)$ with $\mathbb{T}^2$ is a single real point. □

The above technique applies also to the spectral curve of the Ising model (not necessarily ferromagnetic) with $k \times 1$ periodicity on the triangular lattice. The details are omitted.

Proposition 10.3. *Consider a periodic Ising model on the triangular lattice. To each edge e, associate a coupling constant $J_e \in \mathbb{R}$. Assume the coupling constants are translation-invariant with period $k \times 1$ where $k \geq 1$. The only possible intersections of the spectral curve with the unit torus are real points.*

Example 10.4. *Here is an example which explores the generality of the arguments of the current paper, when compared to* [29]. *We start with an Ising model on the triangular lattice $\mathbb{T}$, with edge interactions $J_e \in \mathbb{R}$ that are periodic with period 2×1. Let $\mathbb{H}$ be the dual hexagonal lattice of $\mathbb{T}$. The corresponding Fisher graph $\mathbb{F}$ is obtained from $\mathbb{H}$ by replacing each vertex by a triangle. Each triangle edge is assigned weight 1, and a non-triangle edge crossing an edge e of $\mathbb{T}$ has weight e^{2J_e}.*

The dimer model on $\mathbb{F}$ with the above edge-weights corresponds to the Ising model on the triangular lattice. Note that the spins of the Ising model are placed at centres of the dodecagons of $\mathbb{F}$. Two adjacent spins have the same state (respectively, opposite states) if and only if the corresponding non-triangle edge of $\mathbb{F}$ separating the two dodecagons are present (respectively, absent).

See Figure 10.2 for an illustration, where $a_1, b_1, c_1, a_2, b_2, c_2$ are the edge-weights e^{2J_e}.

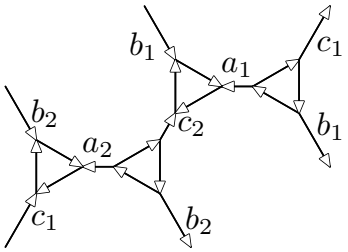

FIGURE 10.2. The Fisher graph with 2×1 periodic edge weights

Given the clockwise-odd orientation of Figure 10.2, we can compute the characteristic polynomial $P(z, w) = \det K(z, w)$, where $K(z, w)$ is the modified weighted adjacency matrix whose rows and columns are indexed by vertices in the 2×1 fundamental domain. By Corollary 10.3, when $a_1, b_1, c_1, a_2, b_2, c_2 > 0$, the only possible intersection of $P(z, w)$ with the unit torus are real.

The function $P(z, w)$ may be calculated as in Section 5.2, and it may be checked that, when $(a_1, b_1, c_1, a_2, b_2, c_2) = (1.1, 0.9, 0, 0, 0.5, 0.5)$,

$$P(1,1)P(1,-1)P(-1,1)P(-1,-1) \neq 0. \tag{10.5}$$

Let $(a_1, b_1, b_2, c_2) = (1.1, 0.9, 0.5, 0.5)$ and assume that c_1, a_2 are positive and sufficiently small that (10.5) continues to hold. By Proposition 10.3, the spectral curve does not intersect the unit torus. As in [3, 8, 22], *the Ising free energy may be expressed in the form (6.10). However, when $(a_1, b_1, b_2, c_2) = (1.1, 0.9, 0.5, 0.5)$ and*

c_1, a_2 are positive and sufficiently small, then neither the high-temperature nor the low-temperature condition of [29] *is satisfied.*

Moreover, using the technique of [24]*, the square of the spin–spin correlation may be expressed as the determinant of a block Toeplitz matrix. By applying similar techniques as in Sections 8–9, we can obtain the convergence rate of the spin–spin correlation of the Ising model of* (10.1) *whenever the spectral curve does not intersect the unit torus.*

10.3. **Harnack curve.** We present next another sufficient condition for the spectral curve $P(z,w)=0$ to intersect the unit torus at only real points. The exponential convergence rate for two-edge correlation functions follows by Theorem 10.1.

Harnack curves were studied in [30, 31]. Simply speaking, a Harnack curve is the real part of a real algebraic curve A (real zeros of a Laurent polynomial with real coefficients) such that the map (10.6) from A to $\mathbb{R}^2$ is at most two-to-one. It was proved in [21, 22] that the spectral curve of any positive-weight, bi-periodic, planar, bipartite dimer model is a Harnack curve. Using the combinatorial results of [9], we infer that the spectral curve of any ferromagnetic, bi-periodic, planar Ising model is also a Harnack curve. If the Ising model is not ferromagnetic, there may exist a concrete counterexample in which the spectral curve is not Harnack, [18]. We give here a simple proof that, under certain conditions, the assumption that the spectral curve is Harnack implies that its intersections with the unit torus are necessarily real.

Proposition 10.5. *Let $P(z,w)$ be a Laurent polynomial taking real values on the unit torus. If $A:=\{(z,w)\in\mathbb{C}^2 : P(z,w)=0\}$ is a Harnack curve, then A can only intersect the unit torus $\mathbb{T}^2$ at real points.*

Proof. Define the logarithmic Gaussian map $\gamma_P : A\to\mathbb{C}P^1$ by

$$\gamma_P(z,w)=\left(z\frac{\partial P}{\partial z}, w\frac{\partial P}{\partial w}\right),$$

and also $\mathrm{Log}:A\to\mathbb{R}^2$ by

$$\mathrm{Log}:(z,w)\mapsto(\log|z|,\log|w|). \tag{10.6}$$

By [30, Lemma 5], A is Harnack, whence the real zeros satisfy $A\cap\mathbb{R}^2=\gamma_P^{-1}(\mathbb{R}P^1)$. By [30, Lemma 3], $\gamma_P^{-1}(\mathbb{R}P^1)$ consists of the singular points of the map Log.

Let $(z,w)=(e^{i\theta},e^{i\phi})\in A\cap\mathbb{T}^2$. Since $P(z,w)$ is a Laurent polynomial, we have that

$$\frac{\partial P}{\partial\overline{z}}=0,\qquad \frac{\partial P}{\partial\overline{w}}=0,$$

and hence

$$\gamma_P(z,w)=\left(i\frac{\partial P}{\partial\theta}, i\frac{\partial P}{\partial\phi}\right).$$

Given that P takes real values on $\mathbb{T}^2$, $\gamma_P(z,w) \in \mathbb{R}P^1$. Hence $A \cap \mathbb{T}^2 \subseteq \gamma_P^{-1}(\mathbb{R}P^1) = A \cap \mathbb{R}^2$. Therefore, any zero of $P(z,w)$ on $\mathbb{T}^2$ is real. □

11. Appendix: Proof of Lemma 7.2

This proof makes use of an elementary lemma concerning monomials, of which the proof is omitted (see [23, p. 176, Cor. 1.6]). Let $x_1, x_2, \dots, x_r$ be independent variables (which for concreteness we may take as real-valued). A *monomial* is a product of the form $\prod_{i=1}^r x_i^{n_i}$ where $n_i \in \{0,1,2,\dots\}$.

Lemma 11.1. *Let $(A_j : 1 \le j \le J)$ and $(B_k : 1 \le k \le K)$ be two sequences of distinct monomials. If*

$$\left| \sum_{j=1}^{J} \alpha_j A_j \right| \equiv \left| \sum_{k=1}^{K} \beta_k B_k \right|, \tag{11.1}$$

where $\alpha_j, \beta_k \in \mathbb{R}\backslash\{0\}$, then there exists $s \in \{-1,1\}$ such that $(\alpha_j A_j)$ is a permutation of $(s\beta_k B_k)$.

Let $A = (a_{i,j})_{1 \le i,j \le 2m}$. By considering A^{-1} in terms of cofactors, we have that

$$\det \widehat{A}_L = \det(A) \det(A_L^{-1}), \tag{11.2}$$

see also [19, p. 601]. Since these matrices are anti-symmetric, they have Pfaffians which satisfy $\mathrm{Pf}\,\widehat{A}_L = \pm \mathrm{Pf}\,(A)\mathrm{Pf}\,(A_L^{-1})$. We shall prove by induction on $\frac{1}{2}|L|$ that

$$\mathrm{Pf}\,\widehat{A}_L = (-1)^{S(L)} \mathrm{Pf}\,(A)\mathrm{Pf}\,(A_L^{-1}). \tag{11.3}$$

Suppose first that $\frac{1}{2}|L| = 1$, and set $L = \{p,q\}$ with $1 \le p < q \le 2m$. Since $A^{-1}_{\{p,q\}}$ is a 2×2 anti-symmetric matrix,

$$\mathrm{Pf}\,(A^{-1}_{\{p,q\}}) = [A^{-1}]_{p,q} = \frac{(-1)^{p+q} \det A^{q,p}}{\det A}, \tag{11.4}$$

where $A^{q,p}$ is the $(2n-1) \times (2n-1)$ submatrix of A after deletion of the qth row and pth column. It suffices for (11.3) that

$$\det(A^{q,p}) = \mathrm{Pf}\,(\widehat{A}_{\{p,q\}})\mathrm{Pf}\,(A), \tag{11.5}$$

and we have already by (11.2) and (11.4) that

$$|\det(A^{q,p})| = \left| \mathrm{Pf}\,(\widehat{A}_{\{p,q\}})\mathrm{Pf}\,(A) \right|. \tag{11.6}$$

Lemma 11.2. *Equation (11.5) holds.*

Proof. We may assume without loss of generality that $p = 1$, $q = 2$. This is so by row/column movements as follows. If $p \neq 1$, the exchange of the columns labelled 1 and p (in addition to the corresponding row on the right side) changes the sign on both sides of (11.5). The same holds for row q (with column q on the right side).

Since each side of (11.5) is continuous in the $a_{i,j}$, we may assume for simplicity that $a_{i,j} \neq 0$ for $i \neq j$. Each term in (11.5) is a sum over monomials in the variables $\{a_{i,j} : i < j\}$, and (11.6) is an identity. By Lemma 11.1, the sets of monomials on the left and right sides of (11.5) are identical, and there exists $s \in \{-1, 1\}$ such that each monomial on the left of (11.4) appears also on the right with the coefficient s. It suffices to show that $s = 1$, and to this end it is enough to consider the sign of any single monomial.

We choose to consider the monomial

$$M = a_{1,2}\big[a_{3,4}a_{5,6}\cdots a_{2m-1,2m}\big]^2,$$

and we shall show, as required, that M has the same sign on the two sides of (11.5). Consider first the left side of (11.5), and recall for illustration that

$$\det A = \sum_{\sigma\in S_{2m}} \operatorname{sgn}(\sigma) \prod_{i=1}^{2m} a_{i,\sigma(i)}, \tag{11.7}$$

where S_{2m} is the set of permutations of $\{1, 2, \dots, 2m\}$. We replace A by $A^{2,1}$ in (11.7), and retain the labelling of rows and columns. The monomial M arises as the product of $m-1$ transpositions (r, s), each of which contributes $a_{r,s}a_{s,r} = -a_{r,s}^2$. The 'aggregate' sign of M is $(-1)^{m-1}(-1)^{m-1} = 1$.

We turn to the right side of (11.5), and recall the definition (7.11) of $\operatorname{Pf} A$ via matchings. The monomial M arises on the right side of (11.5) as the product $M = M'M''$, where

$$M' = a_{3,4}a_{5,6}\cdots a_{2m-1,2m}, \qquad M'' = a_{1,2}a_{3,4}\cdots a_{2m-1,2m}$$

contribute to $\operatorname{Pf}(\widehat{A}_{\{1,2\}})$ and $\operatorname{Pf}(A)$,
resp, By (7.12) or otherwise, the sign of M on the right side of (11.5) is $+$. The proof is complete. □

We have proved (11.3) when $\frac{1}{2}|L| = 1$. We now prove it for general L by induction on $\frac{1}{2}|L|$. Here is the induction hypothesis:

$$H_l : \text{(11.3) is true for } 1 \leq \tfrac{1}{2}|L| \leq l.$$

Let $k \geq 2$, and assume H_{k-1} holds.

Let $L = \{l_1, \dots, l_{2k}\}$, where $l_i < l_j$ if $i < j$. By expanding $\mathrm{Pf}\, A_L^{-1}$ in terms of its first row,

$$\begin{aligned}(11.8)\quad \mathrm{Pf}\,(A_L^{-1})\mathrm{Pf}\,(A) &= \sum_{j=2}^{2k}(-1)^j[A^{-1}]_{l_1,l_j}\mathrm{Pf}\,(A^{-1}_{L\setminus\{l_1,l_j\}})\mathrm{Pf}\,(A)\\ &= \sum_{j=2}^{2k}(-1)^j\mathrm{Pf}\,(A^{-1}_{L\setminus\{l_1,l_j\}})\left[\mathrm{Pf}\,(A^{-1}_{\{l_1,l_j\}})\mathrm{Pf}\,(A)\right] \qquad \text{by (11.4)}\\ &= \sum_{j=2}^{2k}(-1)^{j+l_1+l_j}\mathrm{Pf}\,(A^{-1}_{L\setminus\{l_1,l_j\}})\mathrm{Pf}\,(\widehat{A}_{\{l_1,l_j\}}), \qquad \text{by } H_1.\end{aligned}$$

By H_{k-1}, we have that

$$(11.9)\qquad \mathrm{Pf}\,(A^{-1}_{L\setminus\{l_1,l_j\}}) = (-1)^{S(L)-l_1-l_j}\frac{\mathrm{Pf}\,(\widehat{A}_{L\setminus\{l_1,l_j\}})}{\mathrm{Pf}\,(A)},$$

which we substitute into (11.8) to obtain

$$(11.10)\qquad \mathrm{Pf}\,(A_L^{-1})\mathrm{Pf}\,(A) = (-1)^{S(L)}\sum_{j=2}^{2k}(-1)^j\frac{\mathrm{Pf}\,(\widehat{A}_{L\setminus\{l_1,l_j\}})\mathrm{Pf}\,(\widehat{A}_{\{l_1,l_j\}})}{\mathrm{Pf}\,(A)}.$$

Therefore, in order to prove H_k it suffices to prove that

$$(11.11)\qquad \sum_{j=2}^{2k}(-1)^j\mathrm{Pf}\,(\widehat{A}_{L\setminus\{l_1,l_j\}})\mathrm{Pf}\,(\widehat{A}_{\{l_1,l_j\}}) = \mathrm{Pf}\,(A)\mathrm{Pf}\,(\widehat{A}_L).$$

By (11.2), we have $|\mathrm{Pf}\,(A_L^{-1})\mathrm{Pf}\,(A)| = |\mathrm{Pf}\,(\widehat{A}_L)|$, whence, by (11.10),

$$(11.12)\qquad \left|\sum_{j=2}^{2k}(-1)^j\mathrm{Pf}\,(\widehat{A}_{L\setminus\{l_1,l_j\}})\mathrm{Pf}\,(\widehat{A}_{\{l_1,l_j\}})\right| = \left|\mathrm{Pf}\,(A)\mathrm{Pf}\,(\widehat{A}_L)\right|.$$

Lemma 11.3. *Equation* (11.11) *holds.*

Proof. As in the proof of Lemma 11.2, it suffices to prove that any given monomial appears on the left and right sides of (11.11) with the same sign. As before, we lose no generality by taking $L = \{1, 2, \dots, 2k\}$.

We choose to consider the monomial

$$M = a_{1,2}\cdots a_{2k-1,2k}a^2_{2k+1,2k+2}\cdots a^2_{2m-1,2m}$$

on the right side of (11.11), comprising the product of $a_{1,2}a_{3,4}\cdots a_{2m-1,2m}$ from $\mathrm{Pf}\,(A)$ and $a_{2k+1,2k+2}\cdots a_{2m-1,2m}$ from $\mathrm{Pf}\,(\widehat{A}_L)$. The signs of the two corresponding permutations are $+1$, whence the corresponding sign of M is $+$. The corresponding

monomial on the left side of (11.11) is

$$(-1)^2\big[a_{3,4}\cdots a_{2m-1,2m}\big]\times\big[a_{1,2}a_{2k+1,2k+2}\cdots a_{2m-1,2m}\big],$$

where these two terms are taken from $\mathrm{Pf}\,(\widehat{A}_{\{1,2\}})$ and $\mathrm{Pf}\,(\widehat{A}_{L\setminus\{1,2\}})$, resp, This product also has sign +, and equation (11.11) follows. □

Acknowledgements

This work was supported in part by the Engineering and Physical Sciences Research Council under grant EP/I03372X/1. ZL's research is supported by the Simons Foundation #351813 and National Science Foundation #1608896.

References

[1] P. Billingsley, *Convergence of Probability Measures*, Wiley, New York, 1968.
[2] M. Biskup, *Reflection positivity and phase transition in lattice spin models*, Methods of Contemporary Mathematical Statistical Physics, Springer, Berlin, 2009, pp. 1–86.
[3] C. Boutillier and B. de Tilière, *The critical Z-invariant Ising model via dimers: the periodic case*, Probab. Theory Related Fields **147** (2010), 379–413.
[4] ———, *Statistical mechanics on isoradial graphs*, Probability in Complex Physical Systems (J.-D. Deuschel, B. Gentz, W. König, M. von Renesse, M. Scheutzow, and U. Schmock, eds.), Springer Proceedings in Mathematics, vol. 11, 2012, pp. 491–512.
[5] D. Chelkak, D. Cimasoni, and A. Kassel, *Revisiting the combinatorics of the 2D Ising model*, (2015), http://arxiv.org/abs/1507.08242.
[6] D. Chelkak and S. Smirnov, *Discrete complex analysis on isoradial graphs*, Adv. Math. **228** (2011), 1590–1630.
[7] ———, *Universality in the 2D Ising model and conformal invariance of fermionic observables*, Invent. Math. **189** (2012), 515–580.
[8] H. Cohn, R. Kenyon, and J. Propp, *A variational principle for domino tilings*, J. Amer. Math. Soc. **14** (2000), 297–346.
[9] J. Dubédat, *Exact bosonization of the Ising model*, (2011), http://arxiv.org/abs/1112.4399.
[10] H. Duminil-Copin, R. Peled, W. Samotij, and Y. Spinka, *Exponential decay of loop lengths in the loop $O(n)$ model with large n*, (2014), http://arxiv.org/abs/1412.8326.
[11] M. E. Fisher, *Statistical mechanics of dimers on a plane lattice*, Phys. Rev. **124** (1961), 1664–1672.
[12] I. Gohberg, S. Goldberg, and M. A. Kaashoek, *Classes of Linear Operators, I*, vol. 49, Birkhäuser Verlag, Basel, 1990.
[13] I. C. Gohberg and M. G. Krein, *Introduction to the Theory of Linear Nonselfadjoint Operators in Hilbert Space*, Amer. Math. Soc., Providence, RI, 1969.
[14] G. R. Grimmett, *The Random-Cluster Model*, Springer, Berlin, 2006, available at http://www.statslab.cam.ac.uk/~grg/books/rcm.html.
[15] G. R. Grimmett and Z. Li, *Critical surface of the hexagonal polygon model*, J. Statist. Phys. **163** (2016), 733–753.
[16] W. Kager, M. Lis, and R. Meester, *The signed loop approach to the Ising model: foundations and critical point*, J. Statist. Phys. **152** (2013), 353–387.

[17] P. W. Kasteleyn, *The statistics of dimers on a lattice, I. The number of dimer arrangements on a quadratic lattice*, Physica **27** (1961), 1209–1225.
[18] R. Kenyon, *Private communication.*
[19] ———, *Local statistics of lattice dimers*, Ann. Inst. H. Poincaré, Probab. Statist. **33** (1997), 591–618.
[20] ———, *An introduction to the dimer model*, School and Conference on Probability Theory, ICTP Lect. Notes, XVII, Abdus Salam Int. Cent. Theoret. Phys., Trieste, 2004, pp. 267–304.
[21] R. Kenyon and A. Okounkov, *Planar dimers and Harnack curves*, Duke Math. J. **131** (2006), 499–524.
[22] R. Kenyon, A. Okounkov, and S. Sheffield, *Dimers and amoebae*, Ann. Math. **163** (2006), 1019–1056.
[23] S. Lang, *Algebra*, 3rd ed., Graduate Texts in Mathematics, vol. 211, Springer, New York, 2002.
[24] Z. Li, *Critical temperature of periodic Ising models*, Commun. Math. Phys. **315** (2012), 337–381.
[25] ———, *1-2 model, dimers and clusters*, Electron. J. Probab. **19** (2014), 1–28.
[26] ———, *Spectral curves of periodic Fisher graphs*, J. Math. Phys. **55** (2014), Paper 123301, 25 pp.
[27] ———, *Uniqueness of the infinite homogeneous cluster in the 1-2 model*, Electron. Commun. Probab. **19** (2014), 1–8.
[28] M. Lis, *The fermionic observable in the Ising model and the inverse Kac–Ward operator*, Ann. Henri Poincaré, J. Th. Math. Phys. **15** (2014), 1945–1965.
[29] ———, *Phase transition free regions in the Ising model via the Kac–Ward operator*, Commun. Math. Phys. **331** (2014), 1071–1086.
[30] G. Mikhalkin, *Real algebraic curves, the moment map and amoebas*, Ann. Math. **151** (2000), 309–326.
[31] G. Mikhalkin and H. Rullgard, *Amoebas of maximal area*, Int. Math. Res. Notices **2001** (2000), 441–451.
[32] M. Schwartz and J. Bruck, *Constrained codes as networks of relations*, IEEE Trans. Inform. Th. **54** (2008), 2179–2195.
[33] T. Strohmer, *Four short stories about Toeplitz matrix calculations*, Linear Algebra Appl. **343/344** (2002), 321–344.
[34] H. N. V. Temperley and M. E. Fisher, *Dimer problem in statistical mechanics—an exact result*, Philos. Mag. **6** (1961), 1061–1063.
[35] R. Thomas, *A survey of Pfaffian orientations of graphs*, Proceedings of the International Congress of Mathematicians, vol. III, Europ. Math. Soc., Zurich, 2006, pp. 963–984.
[36] L. G. Valiant, *Holographic algorithms*, SIAM J. Comput. **37** (2008), 1565–1594.
[37] H. Widom, *On the limit of block Toeplitz determinants*, Proc. Amer. Math. Soc. **50** (1975), 167–173.
[38] ———, *Asymptotic behavior of block Toeplitz matrices and determinants. II*, Adv. Math. **21** (1976), 1–29.

Statistical Laboratory, Centre for Mathematical Sciences, Cambridge University, Wilberforce Road, Cambridge CB3 0WB, UK
E-mail address: g.r.grimmett@statslab.cam.ac.uk
URL: http://www.statslab.cam.ac.uk/~grg/

Department of Mathematics, University of Connecticut, Storrs, Connecticut 06269-3009, USA
E-mail address: zhongyang.li@uconn.edu
URL: http://www.math.uconn.edu/~zhongyang/